PHILOSOPHICAL TRANSACTIONS OF THE ROYAL SOCIETY A MATHEMATICAL, PHYSICAL & ENGINEERING SCIENCES

Dimensional Analysis of the Crystal Structures of Intermetallic Phases

W. B. Pearson

Phil. Trans. R. Soc. Lond. A 1980 **298**, 415-449
doi: 10.1098/rsta.1980.0264

DIMENSIONAL ANALYSIS OF THE CRYSTAL STRUCTURES OF INTERMETALLIC PHASES

By W. B. PEARSON

Departments of Physics and of Chemistry, University of Waterloo, Waterloo, Ontario N2L 3G1, Canada

(*Communicated by G. V. Raynor, F.R.S. – Received 25 January 1980*)

CONTENTS

A method of analysing the unit-cell dimensions of crystal structures of binary intermetallic phases is described, that avoids the usual difficulties that result from uncertainty about the appropriate sizes of the atoms, because of their coordination numbers and valencies in the structures considered. Linear equations are obtained that relate the cell dimensions to the atomic diameters for coordination number 12, and sometimes to the valency. These equations permit the explicit identification of the atomic arrays that control the cell dimensions and, therefrom, new quantitative information not previously available, can be derived: for example, (i) the reason for remarkably constant axial ratios of phases of certain uniaxial crystal structures, (ii) the significance of variable or fixed atomic coordinates in relation to structural dimensions, (iii) the fact that, frequently, different atomic arrays control the cell dimensions of phases containing rare-earth atoms, and phases with the same crystal structure that do not contain rare-earth atoms, (iv) the extent to which a system of atomic diameters determined from elemental structures, may be applicable to alloy phases formed by the atoms, and (v) inferences concerning electronic interactions in true interstitial phases.

1. Introduction

Two general problems can be defined in respect of the crystal structures of metallic phases – one chemical: why certain combinations of atoms adopt certain structures, and why the atoms order in certain ways – the other geometrical: why the absolute or relative cell dimensions of a series of phases with a given structure vary in a certain way, why the atoms order as they do, and why certain atoms in a structure have fixed atomic coordinates, whereas some or all of the coordinates of others may be variable.

Existing solutions of the chemical problem are many and they tend to be particular to a single structure, or group of similar structures. An obvious example is phases with the sphalerite structure, the two components of which contribute a total of eight valency electrons, and the adamantine arrangement of which is attributed to the tetrahedrally disposed sp^3 bonds. Other examples involving differences in band-structure energy that are quite small, are the antiphase-domain structures with different out-of-step periods, and the ordered close-packed polytypic structural variations at compositions ML and ML_3, such as were studied by Sato & Toth (1968).

Possible solutions of the geometrical problem would be expected to be more general in nature and to depend on the relative sizes of the component atoms. However, it is for this very reason that no general quantitative solution of the problems is apparent. Since atomic diameter depends both on atomic valency and on atomic coordination, it is uncertain what diameter to adopt when (i) an atom has more than one coordination number (c.n.) in a structure, (ii) the distances from atoms forming a convex coordination polyhedron to the central atom are very disparate and (iii) the valency and/or number of bonding orbitals of an atom in the structure differ from those in its elemental structure from which its diameter was determined – such differences may be serious if they are not apparent. Points (i) and (ii) have perhaps given rise to papers attempting to derive non-integral coordination numbers (cf., for example, the last paragraph in Brunner 1977; Carter 1978). Point (iii) raises the question whether an atomic diameter derived from an elemental structure can be applied effectively to the interatomic distances observed in the structures of metallic phases. For example, Slater (1962) derived a general system of atomic radii applicable to all solids, but through generality this loses effectiveness in specific application. On the other hand, Pauling (1947) was very well aware that metallic radii depended on the bond orbitals involved. Such is the nature of the difficulties involved in a solution of the geometrical problem.

In addition to these difficulties, the conventional parameter against which the variation of physical properties (for example, cell dimensions) of a series of phases with a given structure is assessed – the radius ratio – being a ratio, inhibits explicit interpretation of the results in terms of the sizes of the individual atoms.

2. Method of analysing unit-cell dimensions

Most of the problems discussed above can be avoided by a very simple method of analysing the unit-cell dimensions of binary intermetallic phases that was developed recently (Pearson 1979*a*). The method consists of examining the lattice parameters of a series of binary phases, $M_x L_y$, with the same structure and L or M component, as functions respectively of D_M and D_L, the diameters of the atoms for c.n. 12. In practically all cases studied, the lattice parameters are found to vary linearly with D_M and with D_L. The equations expressing these dependences enable

the identification of the atomic arrays in the structure that control the cell edges. First, it is presumed that only those arrays of atoms that are as close as, or closer than, the appropriate radius sums are likely to exercise dimensional control. Secondly, the expected proportionality of the lattice parameters to D_M and D_L for the arrays, is matched with D_M and D_L dependences established in the equations, so that the controlling array can be explicitly identified. For example, if the equation shows that a depends on 1.4 D_M and the structure contains a f.c. cubic array of M atoms that are in contact, indicating that a should be proportional to $\sqrt{2}\ D_M$, it is obvious that this array controls the unit-cell edge. An array of atoms that involves only one M atom along the cell edge in question, could not normally account for an observed D_M dependence of the cell edge larger than 1.0 D_M. On the other hand, the one M atom that was involved could account for a lesser D_M dependence of the unit-cell edge, say 0.7 D_M, since for many reasons it might not exert its full potential in controlling the cell edge.

By such means it has been possible in practically all structures examined, to assign with certainty the atomic arrays that control the cell edges, although should two arrays jointly control a cell dimension, the method of combining the two expected proportionalities is still to be determined. Not all phases with a given structure necessarily have their cell edges controlled by the same atomic arrays, and the rare-earth phases, for example, frequently have cell edges controlled by atomic arrays different from those of the remainder of phases with the same structure.

The justification for this method of analysis lies in the presumption of the validity of Pauling's (1947) equation†, $R(1) - R(n) = 0.30 \lg n$, where n is equal to the atomic valency divided by the coordination number. In this case the coordination numbers of the M and L atoms in the structure studied are not significant, as a change of diameter from c.n. 12 to any other c.n., merely adds or substracts a constant term to the equations that relate the unit-cell dimensions to D_M and D_L.

There are two other assumptions implicit in the method: (i) that the valency and/or number of bond orbitals of atoms in phases examined, are the same as in their elemental structures from which their c.n. 12 diameters are determined, and (ii) that the distribution of the valency electrons between an atom and its neighbours is in accordance with the requirements of Pauling's (1947) equation and the distances between the atoms. Should either of these assumptions prove invalid, 'valency effects' may become apparent in the dependence of the lattice parameters on D_M or D_L, if the appropriate contacts control the cell dimensions. In such a situation, instead of, for example, the a values of all phases, plotted against D_M, lying on a single line, phases with M atoms of valency 1, 2, 3, ..., lie on a series of parallel lines. Such valency effects are but an artefact of the method of analysis, but where they have been observed, they could generally be interpreted quantitatively to give information on the difference of valency states of the atoms in their elemental structures and the structure examined.

In this paper structural and lattice parameter data for phases are taken from Pearson (1967) and from later volumes of *Structure Reports* of the International Union of Crystallography. Atomic

† Pauling's equation is seen not to hold for changes of valency of the rare-earth metals (Teatum *et al.* 1960) and of the actinides (Zachariasen 1973), but it may still hold for a change of coordination of these metals. Furthermore, Teatum *et al.* (1960) have shown that a percentage change of size, rather than a constant change, accompanies the change from c.n. 8 for the b.c. cubic to c.n. 12 for the f.c. cubic structure. However, unless the phases examined cover a very large range of D_M or D_L values, the difference between a constant change of size as predicted by Pauling's equation and a percentage change on going from one c.n. to another, is not likely to be noticed compared to the general scatter of measured lattice parameters due to compositional differences, accuracy of measurement, etc.

PHILOSOPHICAL TRANSACTIONS OF THE ROYAL SOCIETY A MATHEMATICAL, PHYSICAL & ENGINEERING SCIENCES

diameters for c.n. 12 are those given by Teatum *et al.* (1960); rare-earth diameters for c.n. 12 used in figures 13, 15, 16, 18 and 20–22 are those used in Pearson (1980*c*).

The paper first gives examples of the use of the analysis to show why phases with several uniaxial crystal structures have very constant axial ratios. Next it considers three structural features that have been revealed by the analyses: (i) the significance of fixed or variable atomic positions in relation to changing cell dimensions, as the sizes of the component atoms change, (ii) the different dimensional behaviour of phases containing rare-earth atoms, that is frequently observed, compared to phases with the same crystal structure that contain other atoms, and (iii) the valency effects referred to above. Finally the unique dimensional behaviour of phases with the $AlCr_2C$ structure is analysed to give information on the nature of Hägg interstitial phases.

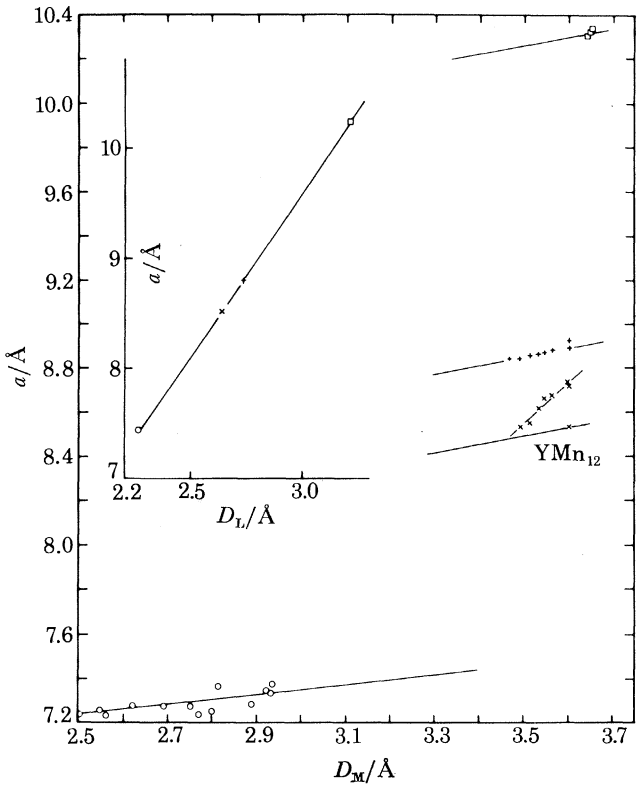

FIGURE 1. $ThMn_{12}$ structure, ML_{12}. Lattice parameter a against the c.n. 12 diameter, D_M, of the M atoms. The inset gives the variation of a with D_L at a constant D_M value of 3.35 Å. Symbols represent alloys of different L components as follows: ○, Be; ×, Mn; +, Zn; □, Mg.

3. PHASES WITH CONSTANT AXIAL RATIOS

To illustrate the method of analysis, we shall show why there is almost no variation of the axial ratio for phases with three different uniaxial crystal structures: the tetragonal $ThMn_{12}$ type, the rhombohedral Th_2Zn_{17} type (hexagonal cell) and the hexagonal Na_3As type.

Figures 1 and 2 show the variation of a and of c with D_M for phases with the $ThMn_{12}$ structure, ML_{12}, and the inserts show the variation of a and of c with D_L at a constant D_M value of 3.35 Å†. Ignoring at present the manganese phases of the rare earths, both the a and c parameters are

† Å = 10^{-10} m = 10^{-1} nm.

virtually independent of the diameter of the M atoms, but depend strongly on the diameter of the L atoms according to the equations

$$a = 3.00\, D_{\mathrm{L}} + 0.610, \tag{1}$$

$$c = 1.74\, D_{\mathrm{L}} + 0.354. \tag{2}$$

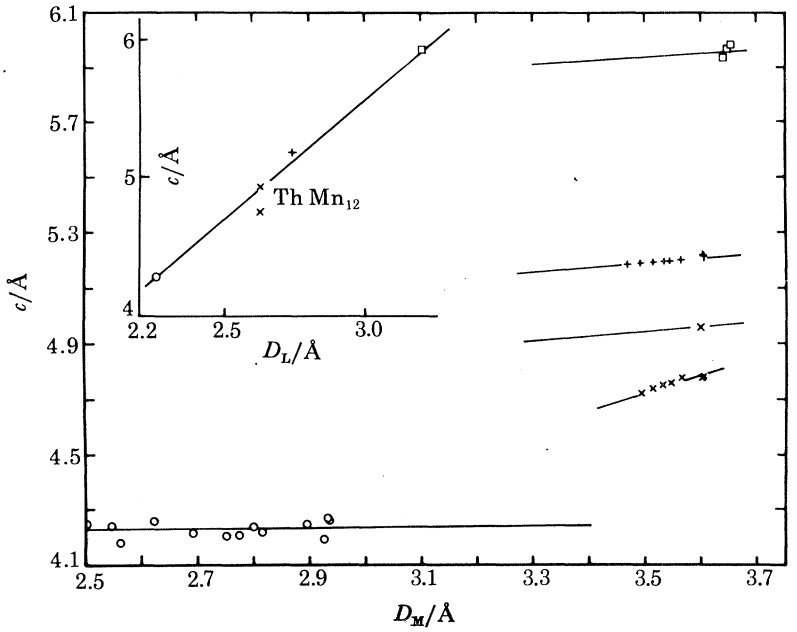

FIGURE 2. As figure 1, except that the c parameter is involved.

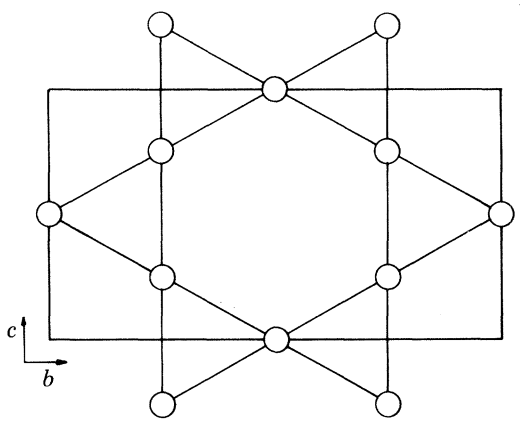

FIGURE 3. $ThMn_{12}$ structure. View of the Kagomé net of Mn atoms and unit cell projected on the (100) plane.

Such behaviour indicates that both cell dimensions are controlled by arrays of L atoms only. These are clearly the interpenetrating Kagomé nets of L atoms in (100) planes at $x = \pm\frac{1}{4}$ and in (010) planes at $y = \pm\frac{1}{4}$. Figure 3 shows the distribution of the atoms on one of these nets relative to the edges of the unit cell. From this it can be seen that a should be proportional to $2\sqrt{3}D_{\mathrm{L}}$ and c to $2D_{\mathrm{L}}$, whence c/a should be approximately 0.577, whereas dividing (2) by (1) gives $c/a =$ 0.580, almost exactly. These values agree so well with the average observed value of 0.582

(maximum deviations $+0.006$, -0.012) for twenty-four MBe_{12}, MMg_{12} and MZn_{12} phases, that it is obvious, that the very constant axial ratio results from the interlocking Kagomé nets of L atoms that control the cell dimensions (Pearson 1980*a*). The influence of the M atom on the unit-cell dimensions is very slight, even though it increases in diameter by 1.15 Å across the series of twenty-four phases.

The remarkable constancy of the axial ratio of the equivalent hexagonal cell of the Th_2Zn_{17} structure, which varies by no more than ± 0.008 from 1.460 for forty-three known phases with

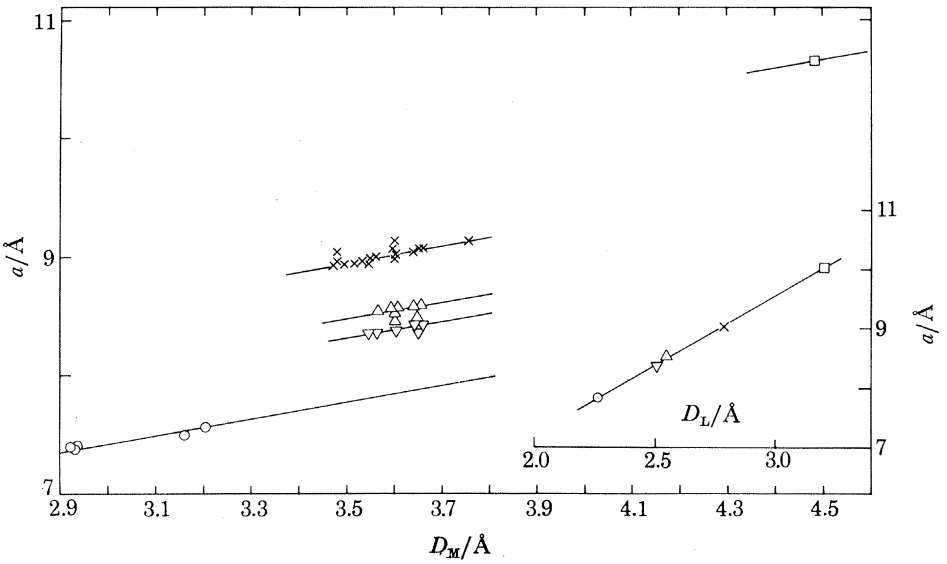

FIGURE 4. Th_2Zn_{17} structure, M_2L_{17}. Lattice parameter a against the c.n. 12 diameter, D_M, of the M atoms. The inset gives the variation of a with D_L at a constant D_M value of 3.6 Å. Symbols represent alloys of different L components as follows: ○, Be; ▽, Co; △, Fe; ×, Zn; □, Mg.

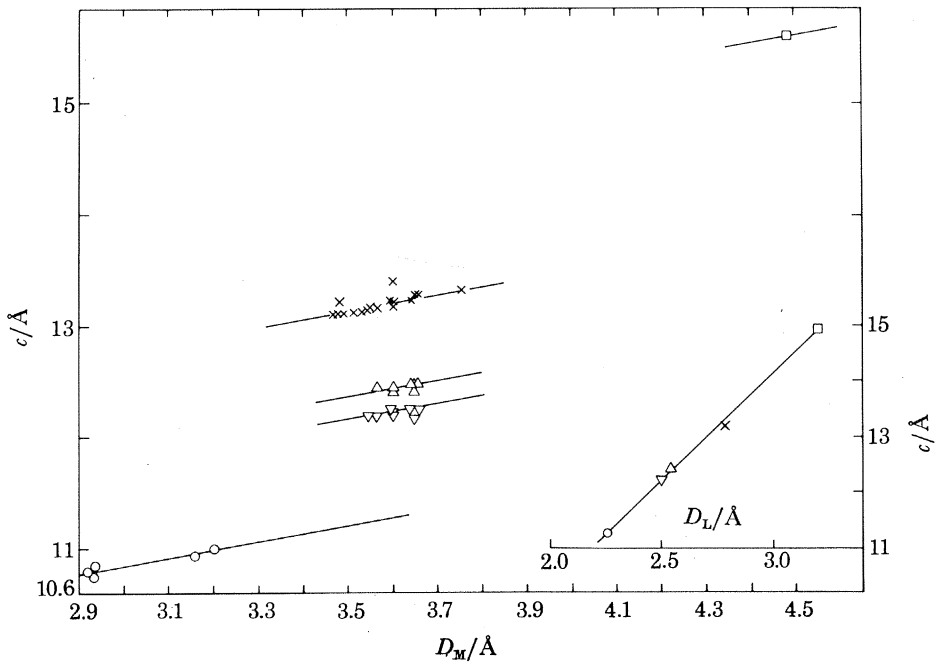

FIGURE 5. As figure 4, except that the c parameter is involved.

this structure (Johnson *et al.* 1969), is a continuing source of wonder, for a metallic phase that has thirty-eight atoms in the unit cell. Figures 4 and 5 show the variations of both a and c with D_{M}, and with D_{L} at a constant D_{M} value of 3.6 Å, which give rise to the equations

$$a = 0.727D_{\mathrm{M}} + 2.286D_{\mathrm{L}} + 0.079, \tag{3}$$

$$c = 0.727D_{\mathrm{M}} + 3.846D_{\mathrm{L}} - 0.010. \tag{4}$$

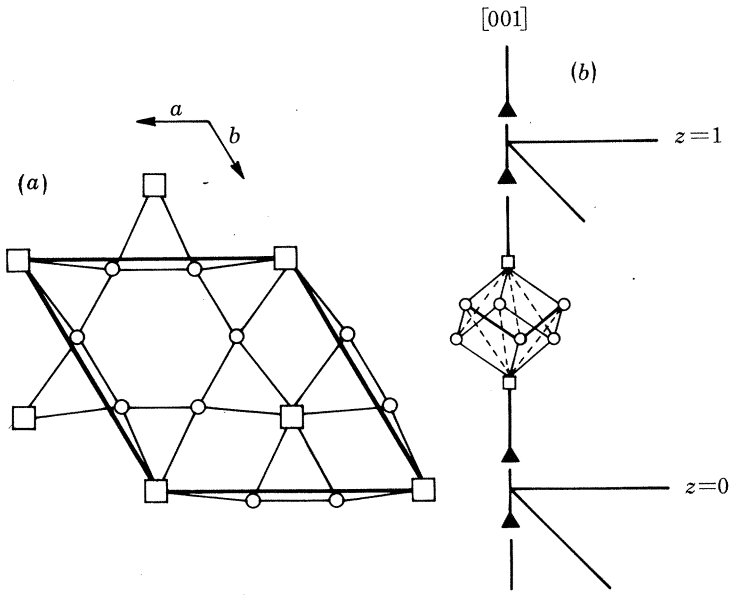

FIGURE 6. Th_2Zn_{17} structure, M_2L_{17}. (*a*) Slightly rumpled hexagon–diamond–triangle arrays of M (□) and L (3) (○) atoms about (0001) planes at $z = 0$, $\frac{1}{3}$ and $\frac{2}{3}$. Layer about $z = \frac{1}{3}$. (*b*) Lines of L(1)–L(1)–M–L(4)–M–L(1)–L(1) atoms along [0001]. □, M atoms; ▲, L(1) atoms; ○, L(4) atoms.

The identical D_{M} dependence of a and c, even though c is some 50 % larger than a, excludes control of the cell dimensions by M atoms in atomic arrays that do not lie along the directions of the unit-cell axes, that is in [0001]- and $\langle 10\bar{1}0\rangle$-type directions. There is only one array along each of these directions that involves both M and L atoms and in which the interatomic contacts are as small as, or smaller than, the appropriate radius sums. In (0001) planes at $z = 0$, $\frac{1}{3}$ and $\frac{2}{3}$ there are hexagon–diamond–triangle nets of M and L atoms, such that M–L–L–M lines of atoms are approximately along the $\langle 10\bar{1}0\rangle$ directions (figure 6). Thus the M dependence of a involves a single diameter of the M atom. Since the a and c dependences on D_{M} are identical, the M dependence of c should also involve a single diameter of the M atom. The only array that could meet this condition consists of [0001] chains of M–L–L–M atoms that are connected by a cage of six L atoms located between the M atoms (figure 6). Since the M–L–L–M portion of the chain already involves a single diameter of the M atom, the $-\mathrm{M}-(\underset{\text{cage}}{\mathrm{L}})-\mathrm{M}-$ portion of the array must be independent of D_{M} and depend only on D_{L}. This condition appears to be met satisfactorily since the distance between the M atoms varies linearly with D_{L}, but somewhat randomly with D_{M}. Of the six phases with the Th_2Zn_{17} structure, the atomic parameters of which have been accurately determined, only two have the same L component. Nevertheless, the linear D_{L} dependence of the M–M distance can be used to correct for the influence of the L atoms of different sizes. Thus table 1 shows that the M–M distances adjusted to a constant D_{L} value of

2.8 Å, vary by less than 0.1 Å, while D_M varies by 1.5 Å, so the condition of the independence of the [0001] M–M cage distance on D_M is well met. Hence the arrays that control the unit-cell edges and the dependences of a and c on D_M and D_L are established. However, dividing (4) by (3) does not give a constant value for c/a, and the reason for the constant axial ratio is to be found in a strong correlation that exists between c/a and D_M/D_L, the diameter ratio of the atoms. Figure 7 shows lines of constant c/a and constant D_M/D_L values on a diagram of D_M against D_L. These run almost parallel to each other. From the figure it can be seen that for phases having observed diameter ratios lying between 1.24 and 1.46, c/a can not vary by more than ± 0.01 from 1.460, as observed (Pearson 1979*a*).

TABLE 1. PHASES WITH THE Th_2Zn_{17} STRUCTURE

phase	M–M distance/Å	D_M/Å
Nb_2Be_{17}	4.327	2.936
U_2Zn_{17}	4.309	3.55
Th_2Fe_{17}	4.318	3.596
Th_2Co_{17}	4.313	3.596
Pr_2Fe_{17}	4.297	3.656
Ba_2Mg_{17}	4.387	4.486

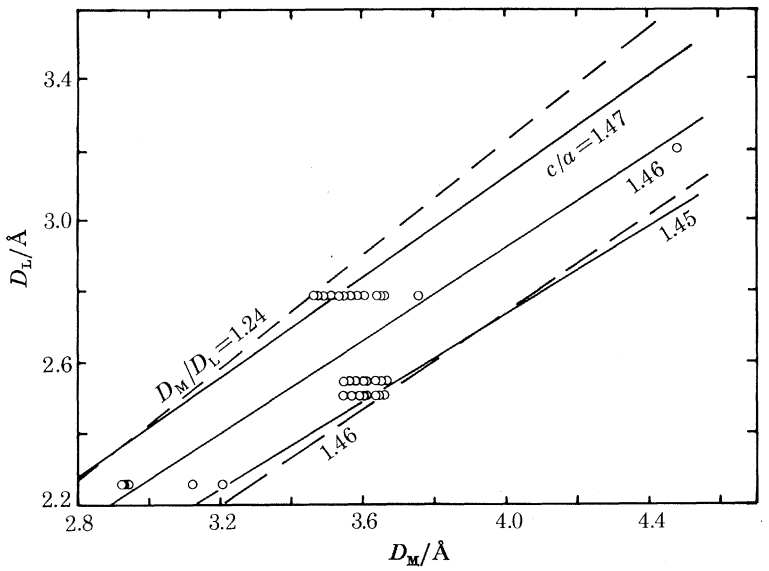

FIGURE 7. Phases with the Th_2Zn_{17} structure. Contours for axial ratios c/a = 1.45, 1.46 and 1.47 as a function of D_M and D_L (——) and constant diameter ratios D_M/D_L = 1.24 and 1.46 (– – –). Also shown are phases having the Th_2Zn_{17} structure (○).

There are nineteen phases that certainly have the hexagonal $AsNa_3$ structure, ML_3, although they are probably all semiconductors rather than metals. The average observed axial ratio for these phases is 1.783 with maximum observed deviations of +0.040 and −0.018.

Figures 8 and 9 show a and c against D_M and the insets show a and c against D_L at a constant D_M value. Except perhaps for the Li compounds, the linear dependence of both a and c on D_M and D_L is apparent and gives rise to the equations:

$$a = 0.61D_M + 0.745D_L + 0.57, \quad (5)$$

$$c = 1.086D_M + 1.33D_L + 1.014. \quad (6)$$

These equations scale as the cell edges, so that (6) divides by (5) exactly, to give a constant axial ratio of 1.78, agreeing with that observed. Thus, multiplying equation (5) by 1.78 gives $a = 1.086\ D_M + 1.33\ D_L + 1.015$ which is seen to be almost identical to equation (6) for c. We have previously recognized that the constant axial ratio in this structure results from the (6 + 2) M–L contacts controlling the cell dimensions, the M atoms forming resonating sp^3 bonds with their eight L neighbours (Pearson 1972).

Thus it is possible to account by means of these analyses, for such structural features as the remarkably constant axial ratios in the structures of certain uniaxial crystals.

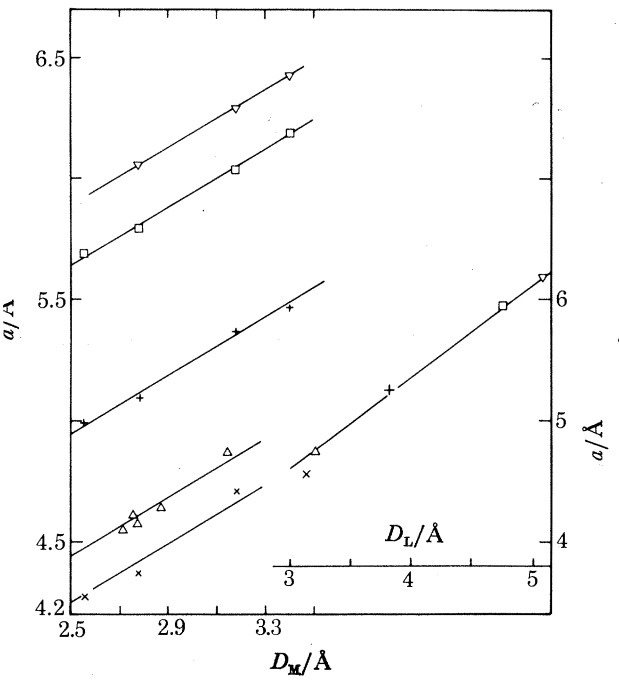

FIGURE 8. $AsNa_3$ structure, ML_3. Lattice parameter a against the c.n. 12 diameter, D_M, of the M components. The inset on the right gives the variation of a with D_L at a constant D_M value of 3.0 Å. Symbols represent alloys of different L components as follows: ×, Li; △, Mg; +, Na; □, K; ▽, Rb.

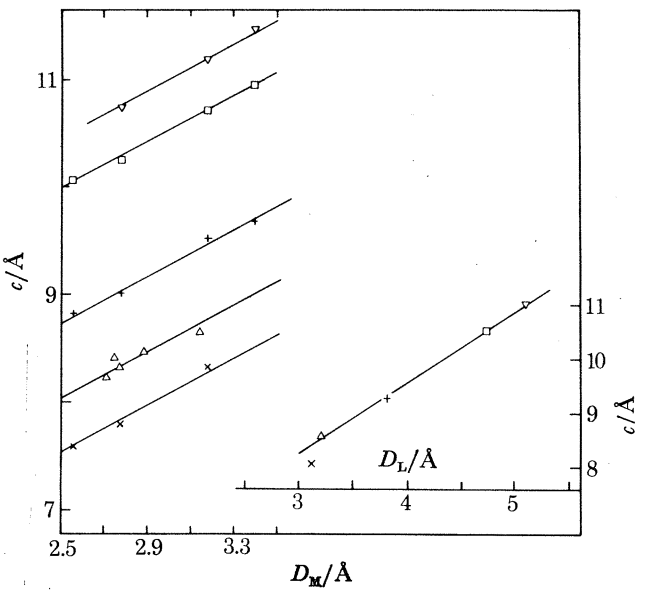

FIGURE 9. As figure 8, except that the c parameter is involved.

4. THE ROLE OF FIXED AND VARIABLE ATOMIC POSITIONS IN CONTROLLING UNIT-CELL DIMENSIONS

There are five independent site-sets occupied by Zn atoms in the Th_2Zn_{17} structure. Only one of these, Zn(2), has completely fixed atomic positions, and it is significant that these atoms are not involved in the two atomic arrays that control the unit-cell dimensions. The Th atoms also have fixed positions, but the other Zn atoms that are in these arrays have variable atomic parameters, x or z, the degrees of freedom of which are either in the directions, $\langle 10\bar{1}0\rangle$ or [0001] that control the cell dimensions, or are transverse to them. Thus the L atoms can adjust their positions in these directions as the relative sizes of the M and L atoms vary in different phases, or can move transversely to these directions to avoid excessive compression of their contacts, should this be necessary. Especially significant is that the L(4) atoms that form the cage of six atoms in close contact

with each other and with the M atoms lying along the [0001] direction, the separation of which is essentially independent of the M atom diameter, can move relatively in $\langle 10\bar{1}0\rangle$ and [0001] directions, to maintain this condition.

It is obvious enough on general principles, that whether the atoms in the crystal structure of a metallic phase have fixed or variable atomic parameters is related to the packing together of atoms of different sizes and bonding characteristics, which determines to a large extent if a phase can adopt a particular crystal structure. However, no particular conditions have previously been recognized in respect of fixed or variable atomic parameters, and the arrays of atoms that control the cell dimensions of crystal structures.

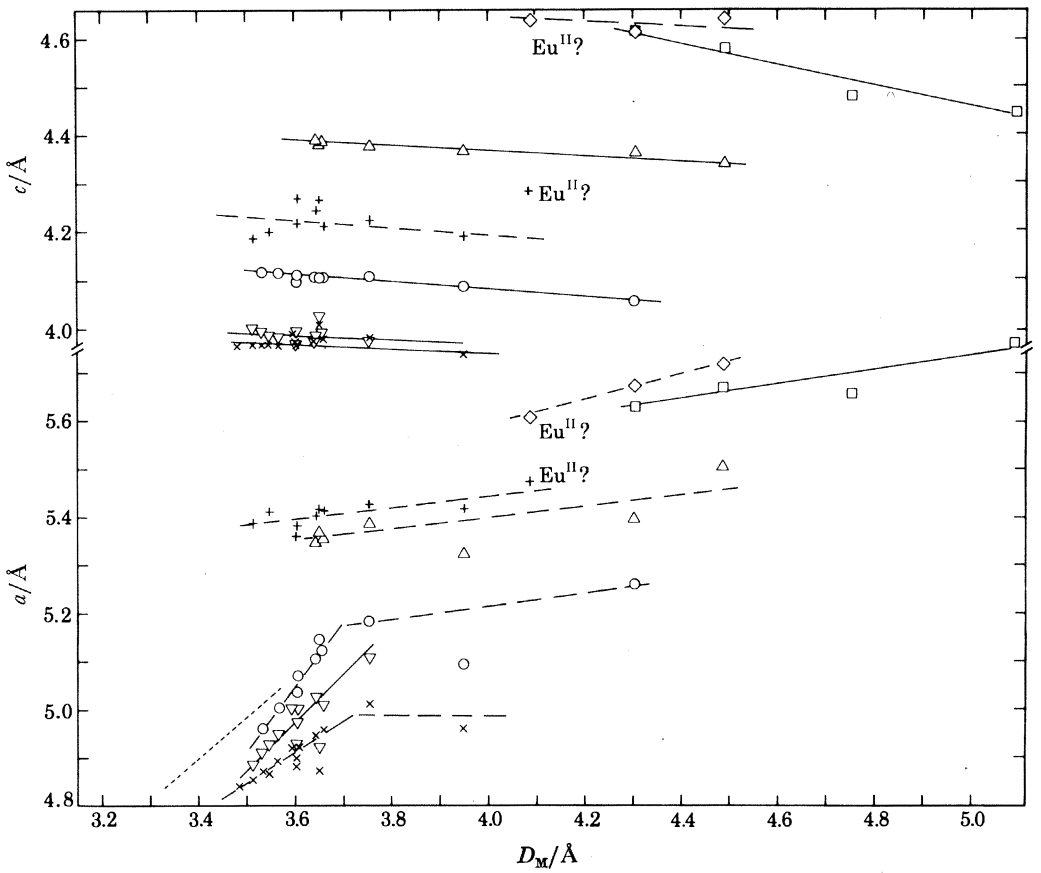

FIGURE 10. Lattice parameters c and a of phases with the hexagonal $CaCu_5$ structure, ML_5, against D_M, the c.n. 12 diameter of the M components. The fine dashed line (------) indicates the calculated slope of the variation of a with D_M, if the M–L contacts in (0001) planes control the a dimension. The following symbols are used for the different L components: ×, Ni; ▽, Co; ○, Cu; +, Zn; △, Pt; □, Au; ◇, Ag.

First, it is apparent that if arrays of atoms involve close M–L, M–M or L–L contacts with interatomic distances equal to, or less than $\frac{1}{2}(D_M + D_L)$, D_M or D_L respectively, and the atoms have fixed fractional coordinates in the structures, the cell dimensions must reflect the changes in atomic diameters between phases, unless the interatomic contacts can be compressed to an indefinite extent. If on the other hand the smaller atoms, say L, in a structure have variable atomic coordinates that permit their movement so as to avoid increasing compression of contacts with their larger M neighbours, as the size of M increases in a series of phases with the same structure and L components, the unit-cell edges may be essentially independent of the size of the M atoms,

as shown in the following. However, observed independence of the cell edges from the diameter of the larger atom, does not necessarily indicate a special significance of variable atomic parameters; it may arise purely from geometrical arrangements in the structure, as in the case of the hexagonal $CaCu_5$ structure which we shall now discuss.

In the $CaCu_5$, ML_5, structure the larger Ca atoms occupy the sites of a simple hexagonal lattice, in the basal planes of which, L(1) atoms form a graphite-like array, so that the M atoms centre the hexagons thereof. Also in (0001) planes, but located at $z = \frac{1}{2}$, the L(2) atoms form Kagomé nets. In the [0001] direction, the L atoms form trigonal bipyramids joined at the apexes of their principal axis, which lies in the [0001] direction. The L–L distances in the trigonal bipyramids and Kagomé nets are as small as, or smaller than their diameters, D_L. As figure 10 shows, it is the trigonal bipyramids of L atoms that control the c dimension of the cell, since c is virtually independent of the diameter of the M atoms and depends on 1.63 D_L. Thus, although the M atoms have fixed positions in the structure, its geometry is such that there is no contact between M atoms along [0001], and the M–L–M arrays of atoms along $\langle 10\bar{1}1\rangle$ directions are also not a dimension-controlling feature.

In the basal plane, with the exception of the Co, Ni, and Cu (also Fe) phases of the rare earths, a is essentially independent of D_M, indicating that the Kagomé nets of L(2) atoms control this cell dimension. The Co, Ni and Cu phases, however, show a distinct dependence on D_M, indicating, since there is also a dependence of a on D_L, that some array of M–L contacts controls a. With c already controlled by D_L, the $\langle 10\bar{1}1\rangle$ M–L contacts could be involved, or the M–L contacts in the basal plane could control a. In the latter case, since both the M and L atoms have fixed positions in the unit cell, and since $D_M > D_L$, the L–L contacts in the $[1\bar{1}00]$ direction, will be unimportant. Only the L–M–L contacts in this direction will be involved in controlling a, so that a should be proportional to $\frac{\sqrt{3}}{2}(D_M + D_L,)$ or to 0.866 D_M. As figure 10 shows, this is about the average slope of a against D_M for the MCo_5, MNi_5, and MCu_5 phases (Pearson 1980*a*).

The significance of this observation, that involves rare-earth phases with transition metals of the first long period, but not rare-earth-zinc or rare-earth-platinum phases, is that strong interactions occur between the rare-earth d and f levels and the 3d levels of the transition metal atoms. The 3d levels for Zn are contracted into the shell and no longer contribute to cohesion or interatomic reactions, as is well proven by the low heat of atomization of Zn compared to that of Cu (Brewer 1965).

To examine the relative importance of variable atomic parameters, we shall consider the $NaZn_{13}$, $BaCd_{11}$ and $BaHg_{11}$ phases, ML_x, in which the M atom is much larger than the L atom (Pearson 1980*b*). On the one hand, since each phase contains less than 10 % of M atoms, their influence on the cell dimensions might be regarded as insignificant. If on the other hand, the M–L contacts are as small as, or smaller than the radius sums, the cell dimensions would be expected to reflect changes of D_M, particularly in the $NaZn_{13}$ structure, where D_M changes by 2.0 Å in the series of phases with L components of Zn and Cd. In fact, allowing for the change of D_L from Zn to Cd, a only increases by about 0.3 Å over this series of alloys.

In the cubic $NaZn_{13}$ structure, the eight Na atoms are located at the centres of each octant at $\pm\frac{111}{444}, \frac{113}{444}\circlearrowleft, \frac{331}{444}\circlearrowleft$, and they are each surrounded by a snub cube of twenty-four Zn(2) atoms. The snub cubes are composed of six squares of four Zn(2) atoms centred on the snub-cube faces that are in {100} planes. They have adjustable x and z parameters that allow their movement in the {100} planes. As the size of the M atom increases in a series of phases with the same L component, the squares of L(2) atoms can expand to accommodate larger M–L(2) distances, without

causing the increase in cell dimensions that would be required if they had fixed coordinates. In the $NaZn_{13}$ structure itself, the Zn(2)–Zn(2) distances forming the edges of these squares on {100} planes are the shortest Zn(2)–Zn(2) contacts on the surface of the snub cube. Thus their expansion with increasing diameter of the M atoms is quite possible, and it makes the different Zn(2)–Zn(2) distances over the surface of the snub cube more nearly equal. The slight dependence of the cell edge on D_M, observed in figure 11 ($a = 0.182D_M + 3.70D_L + 1.369$ for all except the MBe_{13} phases), probably arises through some conflict of L(2) and L(1) atoms, as the squares of L(2) atoms expand. The eight L(1) atoms, located at (000, $\frac{1}{2}\frac{1}{2}\frac{1}{2}$) + (000, $\frac{1}{2}\frac{1}{2}0$ C), are surrounded icosahedrally by twelve L(2) atoms at a distance that, in $NaZn_{13}$, is already smaller than D_{Zn} for c.n. 12.

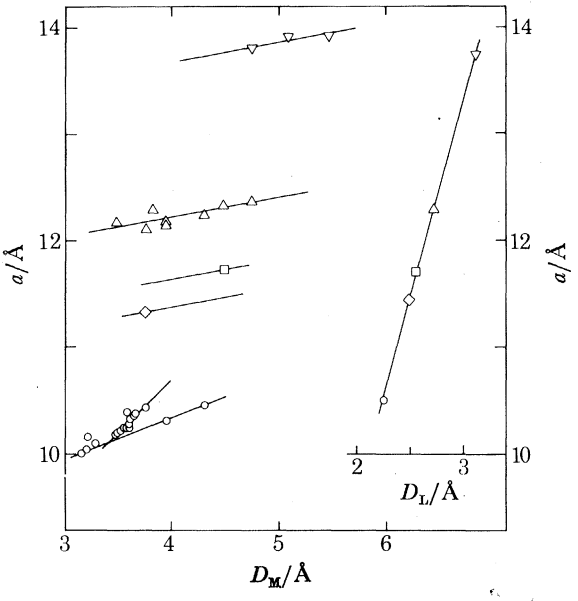

FIGURE 11. $NaZn_{13}$ structure, ML_{13}. Lattice parameter a against D_M, the c.n. 12 diameter of the M component. Inset: variation of a with D_L at a constant value of $D_M = 4.4$ Å. A diameter of 2.74 Å is assumed for Zn. Symbols represent alloys with different L components as follows: ○, Be; ◇, Co; □, Cu; △, Zn; ▽, Cd.

TABLE 2. ATOMIC PARAMETERS AND CERTAIN DISTANCES INVOLVING L(2) ATOMS IN THE $NaZn_{13}$, $MgBe_{13}$ AND $CaBe_{13}$ PHASES.

structure	D_M^*/D_L	y	z	$[\frac{1}{2}(D_M+D_L) - d_{obs}]$/Å	L(2)–L(2) square edge $(D_L - d_{obs})$/Å	other close L(2)–L(2) distances $(D_L - d_{obs})$/Å	$(D_L - d_{obs})$/Å
$NaZn_{13}$	1.435	0.1806	0.1192	−0.198§	0.168	0.058	−0.023
				(−0.174)‡	(0.216)	(0.106)	(0.025)
$MgBe_{13}$	1.500	0.1789	0.1143	−0.160	0.098	0.068	0.00
$CaBe_{13}$	1.830	0.1769	0.1123	0.154	−0.018	0.030	−0.005
$SrBe_{13}$†	1.987	0.175	0.110				

* D_M for c.n. 24, D_L for c.n. 12. † Powder X-ray determination.
§ $D_L = 2.74$ Å, for Zn. ‡ $D_L = 2.788$ Å, for Zn.

Table 2 shows the variation of the x and z parameters and interatomic distances for the three phases with the $NaZn_{13}$ structure, the atomic parameters of which have been determined accurately; they do indeed confirm the description given above, as the diameter ratio, D_M/D_L, of the component atoms increases. It is also seen from the data, that the observed M–L(2) distance

becomes smaller than $\frac{1}{2}(D_M + D_L)$ at a diameter ratio greater than 1.65–1.70. The diameter ratios of the rare-earth phases of beryllium lie in this region, except for the smallest rare earths. It is seen in figures 11 and 13, that the slope of a against D_M for the rare-earth phases of beryllium is notably larger than that for the other phases, a being proportional to $1.0\,D_M$. Thus in phases with a large diameter ratio, such as the rare-earth-beryllium phases, if the x and z parameters of the Be(2) atoms cannot be further altered to separate sufficiently the rare-earth and beryllium atoms, direct dependence of the cell edge on the diameter of the M atom may well result, and is indeed observed.

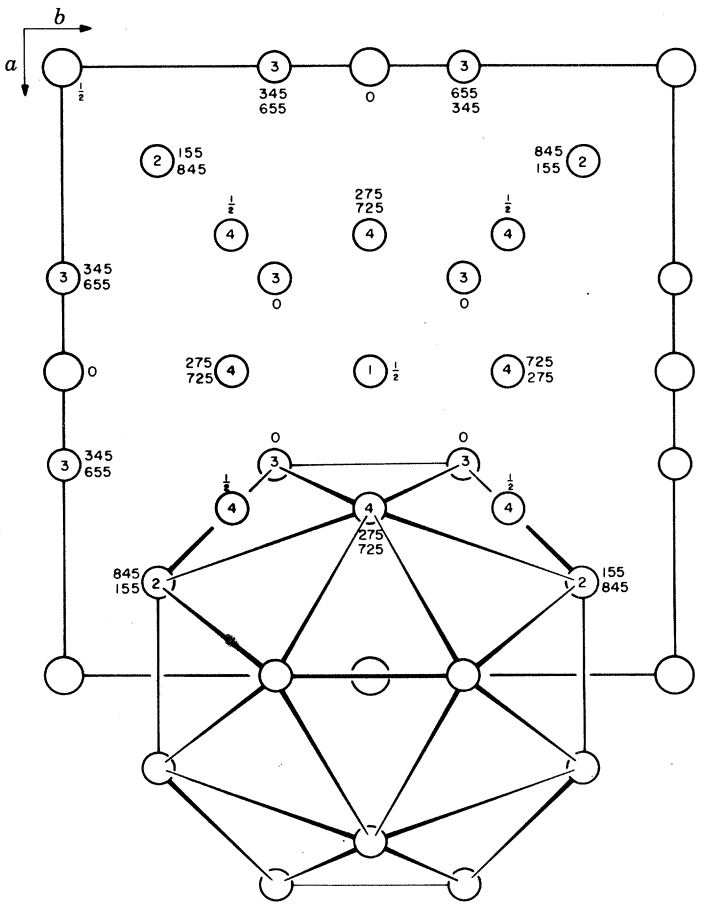

FIGURE 12. The $BaHg_{11}$ structure viewed down [001], showing the coordination polyhedron surrounding Ba (large circles). Numbers indicate fractional coordinates of atoms along [001]; they are $10^3 \times z$-values.

In the hexagonal $BaCd_{11}$ structure, in which the M atoms are surrounded by twenty-two L atoms, a and c are also found to have a relatively small dependence on D_M:

$$a = 0.148D_M + 3.50D_L + 0.368; \tag{7}$$

$$c = 0.071D_M + 2.26D_L + 0.290. \tag{8}$$

The only L atoms common to neighbouring polyhedra are rectangles of L(3) atoms, which, having three variable parameters, can alter their relative positions to accommodate M atoms of increasing size in a series of phases with the same L atom. The L(3) atoms are the closest neighbours of the M atoms in the polyhedra. The other neighbours, the L(1) and L(2) atoms, even

though they have fixed atomic positions, are so far away from the M atom (even in $BaCd_{11}$ which has the largest D_M/D_L ratio of phases with the structure) that their M–L distances do not influence the cell dimensions. Varying the L(3) positions to accommodate larger M atoms, does not influence other atoms in the structure, except for L(3)–L(3) *inter*polyhedra contacts, and these are probably the cause of the weak dependence of observed cell dimensions on D_M.

TABLE 3. RARE-EARTH ALLOYS IN WHICH THERE IS ESSENTIALLY NO DIFFERENCE IN THE SLOPE OF THE CELL PARAMETER AGAINST D_M, COMPARED TO ALLOYS OF THE SAME L COMPONENT THAT DO NOT CONTAIN RARE EARTHS

structure	detail
Th_2Zn_{17}	*a* and *c* for Fe, Co and Zn phases of the rare earths
$ThMn_{12}$	*a* and *c* for Zn (but not Mn) phases of the rare earths
$CaCu_5$	*c* for Co, Ni, Cu, Zn, Pt phases of the rare earths
	a for Zn and Pt (but not Co, Ni and Cu) phases of the rare earths
$BaCd_{11}$	*a* and *c* for Zn phases of the rare earths
$BaHg_{11}$	*a* for Cd phases of the rare earths
CsCl	*a* for Mg and Al phases of the rare earths

In contrast to these two structures, one sees a larger dependence of cell edge on D_M in the cubic $BaHg_{11}$ structure, in which the Ba atoms with fixed positions are surrounded by a polyhedron of twenty Hg(2), Hg(3) and Hg(4) atoms, all of which have variable parameters. The L(3) atoms, which are closest to the M atoms, form squares on {100} planes, and their atomic parameters allow them to move along ⟨110⟩ directions in the {100} planes. However, movement of L(3) atoms along ⟨100⟩ directions to extend the M–L(3) distances and accommodate M atoms of increasing size in a series of phases with the same L atom, shortens the L(3)–L(3) distances in the L(3) squares on {100} planes (figure 12). As these distances are already small (2.976 Å for $BaHg_{11}$, compared to $D_{Hg} = 3.146$ Å for c.n. 12), it is apparent that the cell dimension must be constrained by M–L(3)–L(3)–M lines of atoms on {100} planes. Thus the *a* dependence on D_M given by the equation $a = 0.288D_M + 2.60D_L + 0.100$, is understandably larger than that in the $NaZn_{13}$ or $BaCd_{11}$ phases (Pearson 1980*b*).

Another example is to be found in the $AlCr_2C$ structure discussed in §7 in which the only variable atomic parameter in the structure plays a vital role in linking the dimensions of the *a* and *c* axes of the unit cell.

5. PHASES CONTAINING RARE-EARTH ATOMS

Analyses of the cell dimensions of phases with many structures reveal that the slope of lattice parameter against D_M for c.n. 12 is generally greater for phases of the rare earths (M component) than for those that do not contain rare-earth atoms. However, there are some situations in which the slopes are the same, and these are listed in table 3. Furthermore, with the apparent exception of phases having the orthorhombic FeB structure, phases at the Lu end of the rare-earth series lie on the line of lattice parameter against D_M established for non-rare-earth phases, and phases at the La end of the rare-earth series lie above this line, as shown in figure 13.

This has led to the observation of an empirical atomic-number rule. The lattice parameters of binary phases with the same structure and second component, that are formed by triads of atoms of similar valency, for example, Ca, Sr and Ba, or Sc, Y and La, tend to be a linear function of the

atomic numbers of these atoms, whereas the c.n. 12 diameters of the atoms are not, as indicated in figure 14 (Pearson 1980*c*). For example, the atomic diameter of La for c.n. 12 is 0.168 Å or 4.48 % too small for the atomic diameters of Sc, Y and La to be a linear function of their atomic numbers.

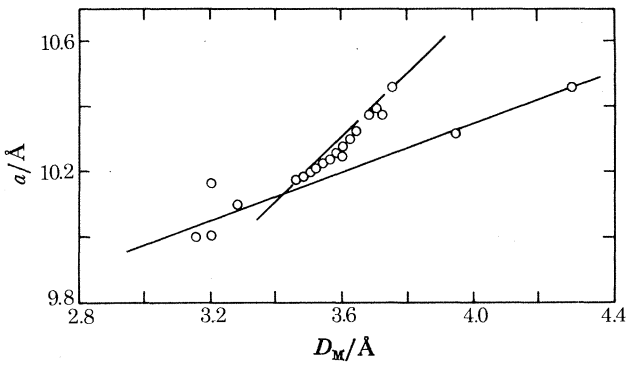

FIGURE 13. Lattice parameter a of MBe_{13} phases with the cubic $NaZn_{13}$ structure against D_M, the c.n. 12 diameter of the M components.

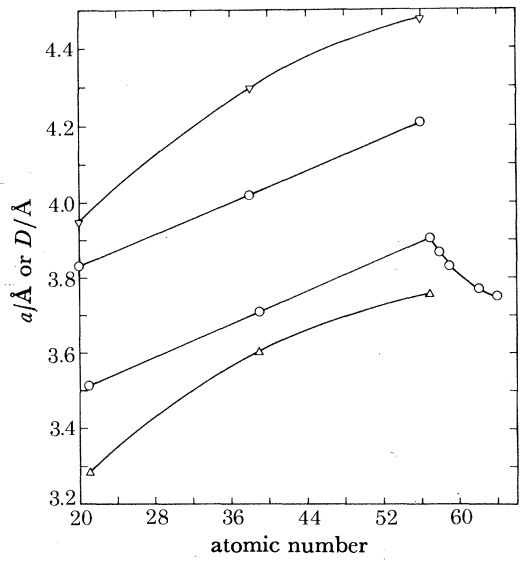

FIGURE 14. Lattice parameter, a, of MCd phases with the CsCl structure plotted against the atomic number of the M component (○). △, Elemental c.n. 12 diameters, D, of Sc, Y and La plotted against their atomic numbers; ▽, elemental c.n. 12 diameters of Ca, Sr and Ba plotted against their atomic numbers.

In support of such an empirical rule, we have twenty-six sets† of lattice parameters for series of Sc, Y and La phases with the same L component in the CsCl, NaCl, $AuCu_3$, $MgCu_2$, $MgZn_2$, CaF_2, $SnNi_3$, CrB, Si_3Mn_5 and $NaZn_{13}$ structures. The mean deviation from linearity of the lattice parameters of these twenty-six sets, as a function of atomic number, expressed as in the foregoing, is |0.046| Å or 0.77 %. By taking account of the sign of the deviation for these twenty-six sets, the average deviation is less than −0.003 Å. Such results appear to be significant in pointing to an empirical rule, that the lattice parameters of these series of phases with the same structure,

† Oxides with the Mn_2O_3 structure, MNi_2 phases with the $MgCu_2$ structure and MB_6 phases with the CaB_6 structure are excluded from these sets, because either there are errors in the measured lattice parameters of some of the phases, or they do not follow the empirical rule.

tend to be a linear function of the atomic numbers of these elements. Whatever the reason for this rule, it is seen to have a definite bearing on the variation of cell dimensions with D_M for rare-earth phases, compared to the variation for phases that do not have rare-earth atoms as the M component.

In view of the findings of this method of analysing the cell dimensions, it would be expected that the lattice parameters of Sc, Y and La, or of Ca, Sr and Ba phases with the same structure and L component, should vary linearly with the atomic diameters of the three elements, for c.n. 12.

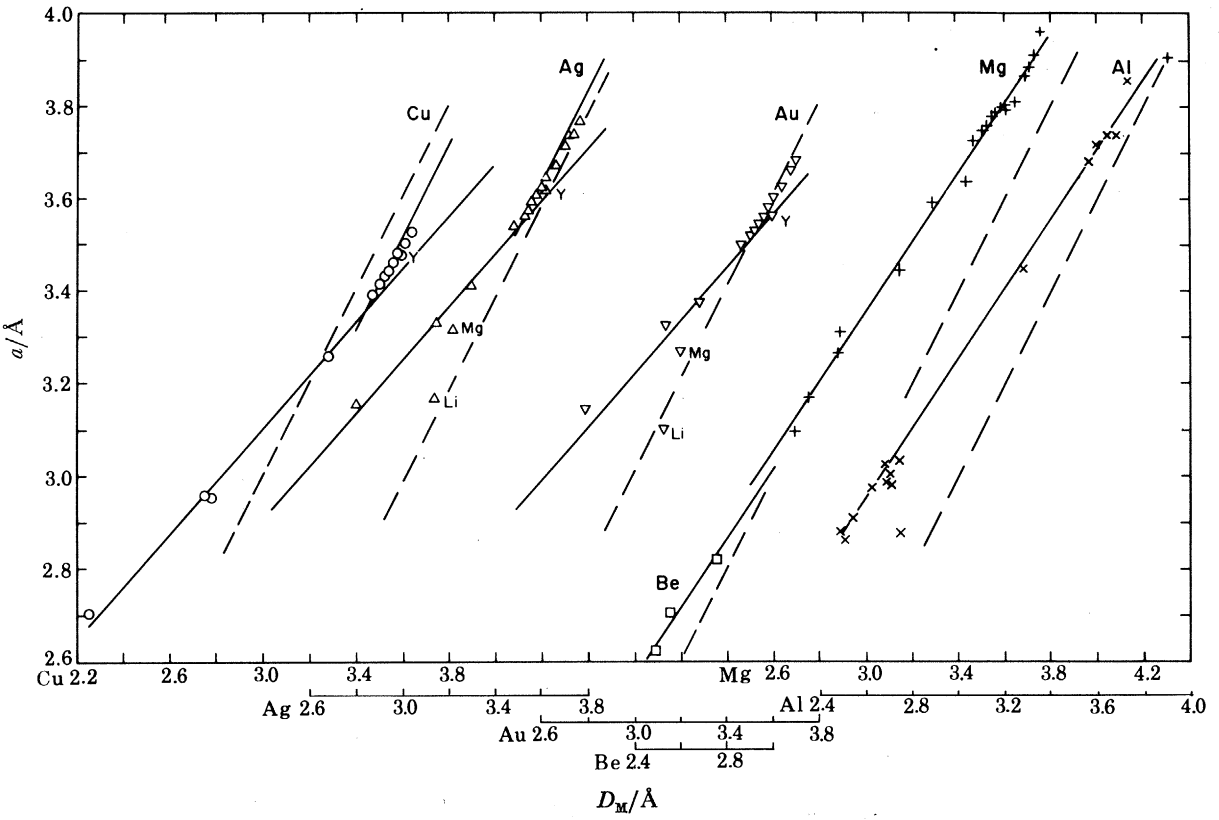

FIGURE 15. Lattice parameter a of phases, ML, with the CsCl structure against D_M, the c.n. 12 diameter of the M components. ---, a against D_M-values that make the M–M distances in the structure equal to D_M. The following symbols are used for the L components: □, Be; +, Mg; ×, Al; ○, Cu; △, Ag; ▽, Au.

However, if the empirical atomic-number rule holds, such an expectation cannot be fulfilled. The c.n. 12 diameter for La would be too small to allow a line joining the Sc_xL_y and Y_xL_y phases on an a against D_M plot, to pass through the La_xL_y phase; indeed, the La_xL_y phase must lie above such a line, as observed in most situations where rare-earth phases are involved. The consequence of this is that in any group of rare-earth phases with the same struture and L component, that obey the empirical atomic-number rule, the rare-earth phases must exhibit a greater dependence of cell edge on D_M, than the non-rare-earth phases, provided that the line for lattice parameter against D_M of the non-rare-earth phases also passes through the points for the Sc_xL_y and Y_xL_y phases. Similarly a Ba_xL_y phase must lie above the line of lattice parameter against D_M joining the Ca_xL_y and Sr_xL_y phases. This is observed for phases with the CsCl, NaCl, CaC_2, $MgZn_2$ and other structures, as indicated for example in figure 16, and the slope of the line joining Sr_xL_y

and $Ba_x L_y$ phases on a lattice parameter against D_M plot is generally similar to that joining the $Lu_x L_y$ and $La_x L_y$ phases in the same system.

In practically all situations where the slope of lattice parameter against D_M is greater for the rare-earth than the non-rare-earth phases, it can be shown that the increased slope results from different atomic arrays controlling the cell dimensions of the rare-earth phases compared to the non-rare-earth phases. One example of such behaviour has already been discussed in §4 for phases with the $CaCu_5$ structure. A similar situation exists in phases with the $ThMn_{12}$ structure, discussed in §3; rare-earth phases with Mn as the L component have different atomic arrays controlling the a and c dimensions compared to those of other phases. We shall now discuss a further example in phases with the cubic CsCl structure.

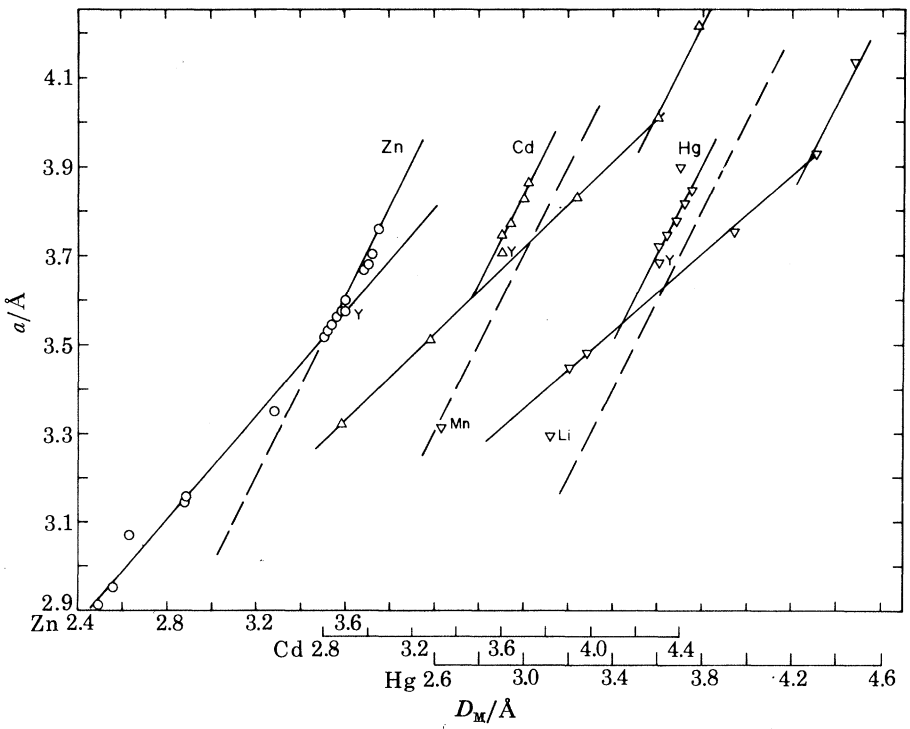

FIGURE 16. Lattice parameter a of phases, ML, with the CsCl structure against D_M, the c.n. 12 diameter of the M components. ---, a against D_M-values that make the M–M distances in the structure equal to D_M. The following symbols are used for the L components: ○, Zn; △, Cd; ▽, Hg.

The cell edge, a, of phases with the CsCl structure is proportional to $0.577D_M$, or slightly less, for non-rare-earth phases with L components, Li, Cu, Ag, Au, Zn, Cd, Hg, Ga, In and Tl, and to 0.8–$1.0D_M$ for their rare-earth phases. However, both rare-earth and non-rare-earth phases of Mg and Al follow an a dependence of about $0.8D_M$ (table 3).

The M–L–M contacts along ⟨111⟩ directions in the CsCl structure are smaller than the radius sums, and they are therefore expected to control the cell dimension. In this situation, a should be proportional to $\frac{1}{\sqrt{3}}(D_M + D_L)$ or to $0.577D_M$ as reported above. The next-nearest contacts in the structure are M–M or L–L contacts along ⟨100⟩ directions, and if either of these control the cell dimension, a should be proportional to $1.0D_M$ or $1.0D_L$, whichever is the larger atom. When M is a rare-earth atom, a is nearly equal to, or less than D_M for c.n. 12 or 14, as indicated in figures 15

and 16. Therefore for these phases the ⟨100⟩ M–M contacts control a, as indicated by the larger dependence of a on D_M for the rare-earth phases, compared to non-rare-earth phases.

Thus it seems clear enough that the increased dependence of a on D_M for the rare-earth phases compared to the non-rare-earth phases, results from M–M rather than M–L–M contacts controlling the cell dimensions. However, it must be asked why phases of the still larger atoms, Ca and Sr, follow the $0.577D_M$ dependence of other non-rare-earth phases; presumably it results from their being relatively open metals thus permitting M–L–M contacts still to control the cell dimensions of their phases. The barium phases, on the other hand, follow the behaviour anticipated from the empirical atomic-number rule. The slope of the line joining Sr and Ba phases is 0.8–$1.0D_M$, similar to that of the rare-earth phases, indicating that ⟨100⟩ Ba–Ba contacts control the cell dimensions of barium phases.

The reason for all phases of Mg and Al having the same cell-edge dependence on about 0.8 D_M, is the result of different interactions in the non-rare-earth, rather than the rare-earth phases, since the D_M dependence is the same as for rare-earth phases of other L components.

In view of the large number of rare-earth phases the structural dimensions of which are controlled by atomic arrays different from the non-rare-earth phases, it is perhaps more cogent to account for those examples listed in table 3, where there is no difference in dimensional control for rare-earth and non-rare-earth phases.

In phases with the $CaCu_5$ structure already discussed in § 4, a is controlled by the Kagomé net of L atoms in the (0001) plane, except for MFe_5, MCo_5, MNi_5 and MCu_5 phases of the rare earths, where control is by L–M–L contacts, also in the (0001) plane, but c is controlled for *all phases* by chains of trigonal bipyramids along the [0001] direction. The reason for this is that there are no arrays involving M atoms that are partly or wholly in the c direction in which the M atoms are in contact with other atoms. In the lines of M atoms in the [0001] direction the M–M separation is much larger than D_M, and in the lines of M–L–M contacts in $(10\bar{1}1)$-type planes, the M–L distances are also greater than $\frac{1}{2}(D_M + D_L)$.

Arrays of M and L atoms already control the cell dimensions of non-rare-earth phases with the Th_2Zn_{17} structure, and as there are no direct M–M interactions in the structure, the same cell-edge dependence on D_M is found for rare-earth and non-rare-earth phases; similarly for phases with the $BaHg_{11}$ structure.

In the $NaZn_{13}$ and $BaCd_{11}$ structures, discussed in the foregoing, the variable position parameters of the L atoms allow their movement to adjust to the changing size of the M atoms, so that there is little M–L interaction and the cell edges show very small D_M dependences. Only when the diameter ratio, D_M/D_L, becomes very large, as in the MBe_{13} phases with the $NaZn_{13}$ structure, does this process become relatively ineffective, resulting in a greater dependence of a on D_M; in particular for the rare-earth phases the M–L distance is approximately equal to, or less than $\frac{1}{2}(D_M + D_L)$. The cell edge, a, is now proportional to $1.0D_M$ (figure 13) and M–L, rather than L–L, contacts control the cell edge. This situation does not exist in MZn_{13} rare-earth phases because the M–L distances are considerably larger than $\frac{1}{2}(D_M + D_L)$.

6. Valency effects observed in analysis of unit-cell dimensions

Normally no valency effects are found in the analyses since atomic diameter expressed for c.n. 12, already takes into account both atomic valency and coordination. If, however, the valency and/or number of bond orbitals used by an atom in the structure under examination, are not the

same as in the elemental structure from which its c.n. 12 diameter was determined, or if the valency electrons of an atom are not distributed in bonds to its neighbours, according to the requirements of the interatomic distances and Pauling's equation, $R(1)-R(n) = 0.30 \lg n$, valency effects may be observed, if the appropriate atomic contacts control the cell dimensions. This is because the elemental D_M or D_L values for c.n. 12, against which the cell dimensions are plotted, will not be correct for the phases studied. Furthermore, since the error in the atomic diameter generally changes with the valency of the component atom considered, the valency

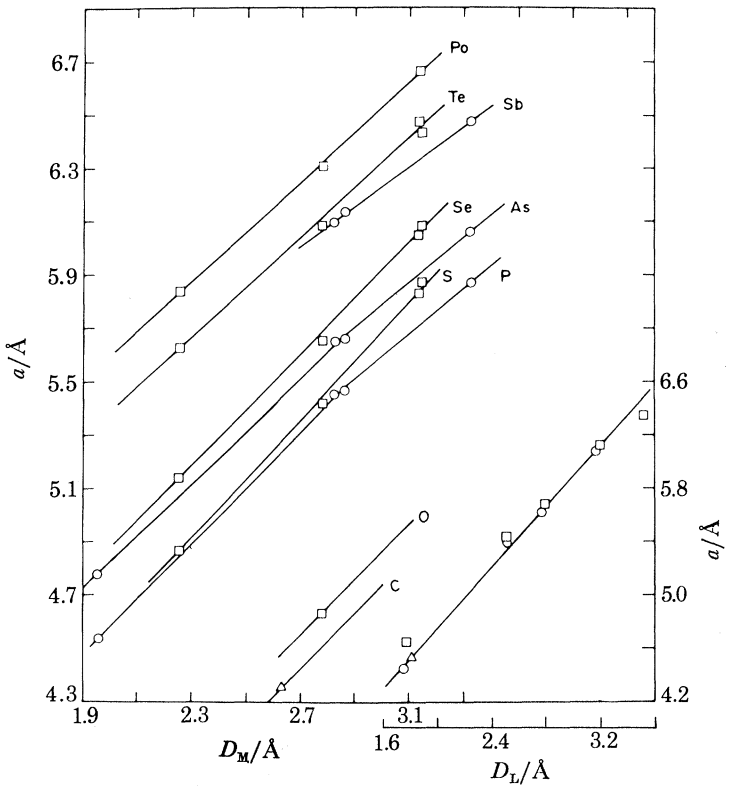

FIGURE 17. Sphalerite, ZnS, structure, ML. Lattice parameter a against c.n. 12 diameter, D_M, of the M component. The L components are named on the diagram and their Group numbers are indicated by symbols: △, IV; ○, V: □, VI. Inset, bottom right: lattice parameter a against c.n. 12 diameter D_L at a constant D_M-value of 2.8 Å.

effect will appear as a series of parallel lines, say of a against D_L, on which L components of valency 1, 2, 3, ... severally lie (figure 19), instead of lying along the single line that occurs when there is no valency effect. Although the effect is an artefact of the method of analysis, it nevertheless detects when the valency of an atom in the structure considered differs from that in its elemental structure, from which its c.n. 12 diameter was determined, provided that the appropriate atomic contacts control the cell dimensions (Pearson 1980*d*).

Electron transfer between the M and L components, resulting from their electronegativity differences would change their effective valencies; this is not expected to be important in phases that are metallic, although it must be considered in the analysis of the dimensions of non-metallic phases. Here, no valency effect will appear if M–L contacts control the cell dimensions, since the increase of electrons on the M atoms can only occur at the expense of the L atoms and vice versa, so changes of lattice parameters on D_M or D_L plots are likely to be too small to be

observable. This is shown in figure 17 for phases with the sphalerite structure, where no valency effects are apparent and the only irregularities concern phases containing indium. This is because the cell edge is controlled by the M–L contacts of the adamantine atomic arrays. For a valency effect to appear in such circumstances it would be necessary for the cell edge to be controlled by arrays of either M–M or L–L atomic contacts.

We shall now give examples of three different types of valency effects that are observed.

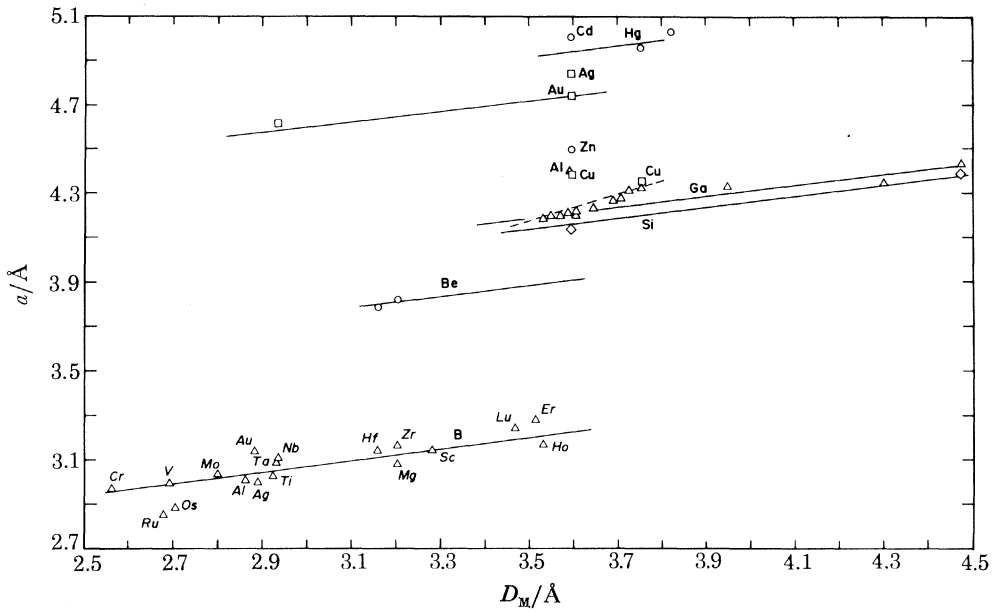

FIGURE 18. AlB_2 structure, ML_2. Lattice parameter a for phases with the AlB_2 structure against D_M, the c.n. 12 diameter of the M component. The L components are named on the diagram, and symbols indicate their valencies: □, valency 1; ○, valency 2; △, valency 3; ◇, valency 4. The M components of MB_2 alloys are also named, but in italic script.

In phases with the hexagonal AlB_2 structure, ML_2, the a cell edge shows little dependence on D_M (figure 18), but is strongly dependent on D_L (figure 19). This results from the graphite-like array of L atoms in (0001) planes controlling the a dimension of the unit cell. There is also a valency effect involving the L atoms (figure 19), which results from a concentration of the L valency electrons in the L–L bonds, at the expense of the M–L bonds. The c edge of the cell shows a linear dependence on D_M, but a random dependence on D_L. It is known from other work (Pearson 1979 *b*) that the c dimension is controlled by M–L contacts that lie in $\langle 20\bar{2}3 \rangle$ directions, the a dimension already being fixed by the L–L contacts. The M–L distances equal $\frac{1}{2}(D_M + D_L)$ to within $|0.05|$ Å for phases, the D_M and D_L values of which are known with certainty.

The valency effect is in the normal sense; that is to say, the larger the valency of the L atom, the shorter is a, except that the effect is greater for L components with valency three than for silicon with valency four. Thus the lines for phases with L atoms of valency two, four, and three are separated from that of phases with valency one by spacings in a of l, $3l$ and $4l$ respectively, where $l = 0.11$ Å (figure 19). The dependence of the a cell dimension on D_M, D_L and S, the valency effect, is given by

$$a = 0.235D_M + 1.19D_L - 0.11S + 0.58, \qquad (9)$$

where S has values 1, 2, 4 and 5 for Group I, II, IV and III L atoms respectively. This equation gives the a values of forty-seven phases with the AlB_2 structure, with an average error of $|0.04|$ Å, from the c.n. 12 diameters of the atoms and the valency of the L atoms alone. As the M–L distances along $\langle 20\bar{2}3\rangle$ are equal to $\frac{1}{2}(D_M + D_L)$, c and c/a can also be calculated from these data alone.

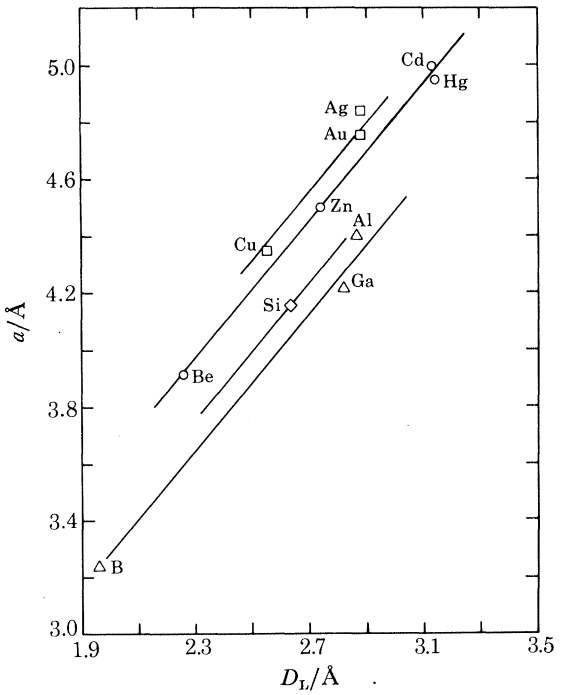

FIGURE 19. AlB_2 structure. ML_2. Lattice parameter a against c.n. 12 diameter, D_L, at a constant D_M value of 3.6 Å. The L components are named on the diagram, and symbols indicating their valencies are as for figure 18.

It is not obvious from (9) why the trivalent elements appear to have a larger valency effect than the four-valent element Si; that is to say, why the trivalent elements have the value $S = 5$, instead of $S = 3$. To understand this requires consideration of the changes of D_L with valency. If there were no valency effects, phases of all L components, regardless of valency, would lie on the same line of a against D_L, and this line would be essentially that of the univalent L components in figure 19. Since, however, the valency electrons are concentrated in the L–L bonds, the elemental c.n. 12 diameters used for the L atoms in figure 19 are incorrect. For the trivalent L atoms, if their three valency electrons were concentrated in the three L–L bonds giving them unit-bond strength, then from Pauling's equation, D_L for the L–L distances should be 0.36 Å smaller than the normal D_L values for c.n. 12. Displacing the line for trivalent elements 0.36 Å to smaller D_L values in figure 19, exactly superimposes it on the line for the univalent L atoms Cu, Ag and Au! If for the L component of valency four, three electrons form three unit-strength bonds to the three L neighbours, and the remaining electron is distributed among the M–L bonds, D_L should be 0.286 Å smaller than its c.n. 12 value. This would also place the line for the element of valency four along that for the univalent elements. Finally, for phases of the divalent L components (and possibly to a small extent for those of the univalent L components), there is some additional concentration of the valency electrons of the L atoms in the L–L bonds, but it is not complete, and some valency electrons remain in the M–L bonds. Thus the larger valency effect of the L

components with valency three compared to that for silicon with valency four, which was for sometime a puzzle (Pearson 1979*b*), can be quantitatively accounted for.

The combination of the valency effect along *a*, and its influence on the *c* parameter through the $\langle 20\bar{2}3\rangle$ M–L contacts and *c*/*a*, is responsible for the two groups of AlB_2 phases on a diagram of *c*/*a* against D_M/D_L which was an unexplained feature of the structure (Pearson 1972, p. 494). The phases of the univalent and divalent L atoms lie close together on such a diagram, corresponding to their *S* values of 1 and 2; similarly phases of L atoms with valency three and four lie close together corresponding to their *S* values of 5 and 4.

'Reverse' valency effects are found for transition metals forming true interstitial phases with H, C and N atoms. They are referred to as 'reverse' because the effect is greatest (lattice parameter smallest) for transition metals of smallest valency – three. Structures and phases showing the effect are generally true interstitial phases with the ratio, radius of metalloid to radius of transition metal of less than 0.59 ($R_L/R_M < 0.59$) and obeying the Hägg rule (1929, 1931). Thus the transition metal atoms generally lie on primitive or face-centred cubic, or simple hexagonal lattices, and the metalloids centre octahedra or tetrahedra of the transition metals in the cubic structures, and trigonal prisms of them in the hexagonal structures. Figures 20, 21, 24 and 25 show these reverse valency effects in transition-metal phases of C and N with the NaCl structure, in dihydrides with the fluorite structure, in phases with the $Si_3Mn_5X_x$ structure, and in carbides with the $AlCr_2C$ structure. Figure 18 indicates the absence of any such valency effect in boride phases with the AlB_2 structure, which are not true interstitial phases, since $R_L/R_M > 0.59$ even though the structural arrangement satisfies the Hägg rule.

The physical basis of the Hägg rule and the reason for these true interstitial phases showing a valency effect, appears to involve the d levels of the transition metals overlapping to form d bands that are not destroyed by the presence of the metalloids when $R_L/R_M < 0.59$. This is in contrast to a normal phase between a transition metal and another atom, where there are no d bands formed between the transition metal atoms. Indeed, recent band-structure calculations, for example those of Neckel *et al.* (1976) for interstitial carbides and nitrides with the rocksalt structure, confirm the formation of transition metal d bands, and their slight overlap with bands formed from metalloid 2p states, which lie at lower energies. However, the transition-metal valency effect may result from nothing more than the average number of valency electrons per transition-metal bond, controlling the cell dimensions in the interstitial phase, adjusted to c.n. 12, differing from that in the corresponding elemental structure from which its c.n. 12 diameter was derived, as shown in § 7. Nevertheless such differences may depend specifically on the possibility of non-bonding electrons existing in the transition-metal d bands.

Figure 20 shows that the cubic cell edge, *a*, depends on about $1.4D_M$ for the interstitial hydrides with the fluorite structure, and the carbides and nitrides with the rocksalt structure, that do not contain rare-earth atoms. This indicates control of the cell dimensions by $\langle 110\rangle$ lines of M–M–M contacts, since *a* would then be expected to be proportional to $\sqrt{2}D_M$. With *a* controlled by M–M contacts, the observed valency effects involving the M transition-metal atoms would be expected, if the average number of electrons per M–M bond differs from that in M–M bonds in their elemental structures, from which their c.n. 12 diameters were determined.

The rare-earth hydrides and nitrides (but not their carbides, which are deficient in C, having a formula M_3C) show a greater dependence of *a* on D_M than the transition-metal phases (figure 20). This appears to be due to the M–L–M chains of atoms acting in conjunction with the M–M–M chains in controlling the cell dimension.

Phases with the hexagonal $Si_3Mn_5X_x$, $L_3M_5X_x$, structure reveal another interesting valency effect. They are reported often to contain and be stabilized by interstitial metalloid atoms located at 000 and $00\frac{1}{2}$ at the centre of octahedra of M(2) atoms. Analysis of the dimensions of these phases suggests that the methods of preparation may result in more frequent occupation of these octahedral holes by interstitial atoms than was generally believed since, as figure 21 shows, the transition metal atoms, M, exhibit reverse valency effects along the a axis of the unit cell. However, little or no valency effect occurs along the c axis of the unit cell (figure 22). The reason for this is that the c dimension of the unit cell is mainly controlled by lines of M(1) atoms in the

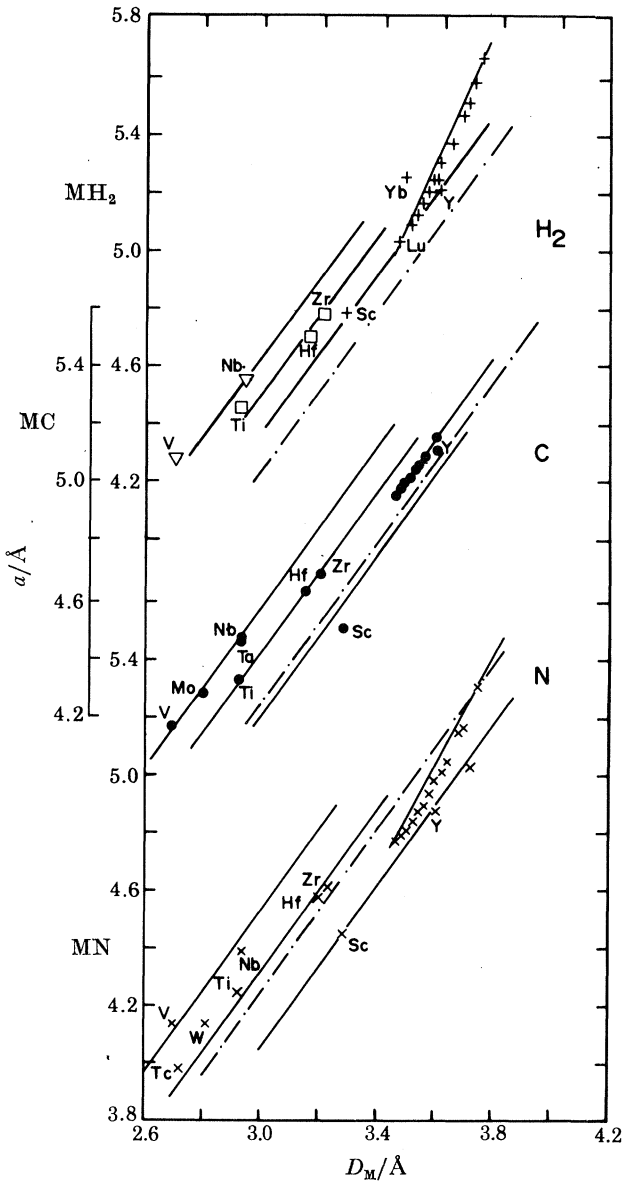

FIGURE 20. Upper: CaF_2 structure, ML_2, of dihydrides. Middle and lower: NaCl structure, ML, of carbides and nitrides (L). The carbides of the rare earths have composition M_3L. Lattice parameter, a, against c.n. 12 diameter, D_M, of the M components that are named on the diagram, except for the rare-earth metals. Full lines drawn with slope of $\sqrt{2}$ join M components of the same valency. –·–, a-values that separate M atoms by a distance equal to D_M.

[0001] direction, thus satisfying the observed c dependence of $1.0D_M$. (In Mn_5Si_3 the M(1)–M(1) distances are 2.407 Å, whereas the M(2)–M(2) and M(2)–L distances, with a component in the [0001] direction, are 2.907 Å and 2.663 Å respectively.) The M(1) atoms are not part of the octahedra of M atoms that are centred by the interstitial atoms. Thus no valency effect is observed along the c axis, whereas it is observed along a, the dimension of which is controlled by arrays of M(2) and L atoms.

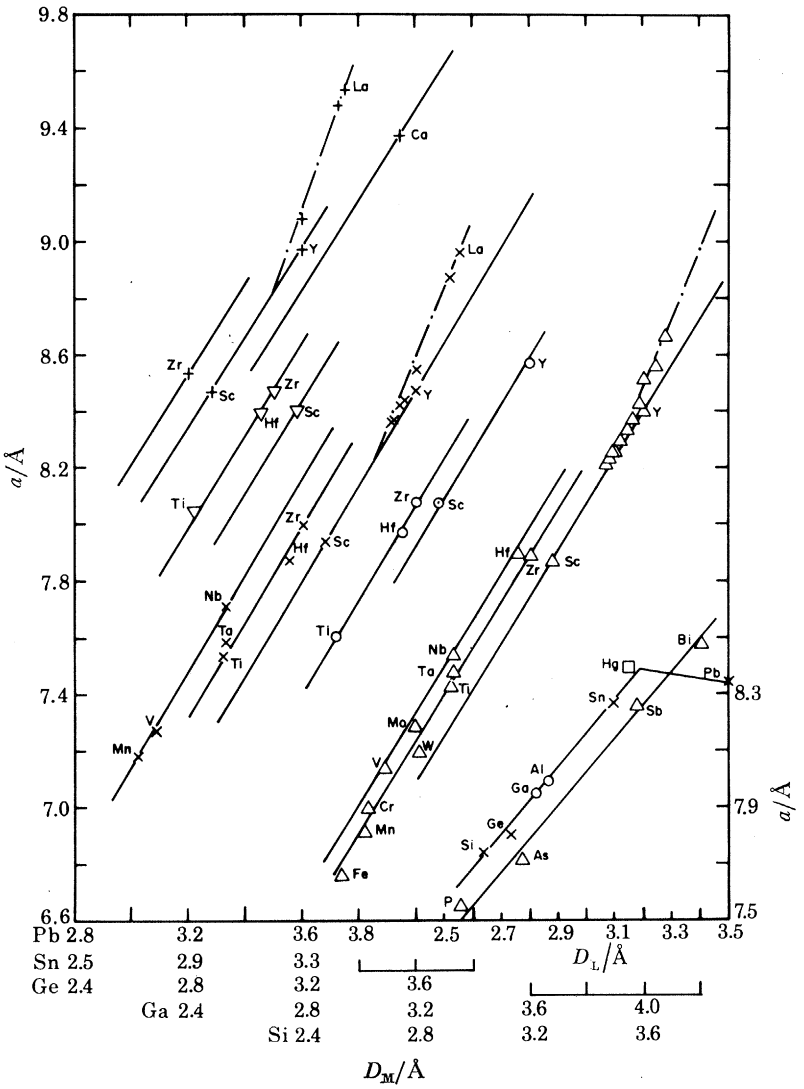

FIGURE 21. $Si_3Mn_5X_x$ structure, $L_3M_5X_x$. Lattice parameter a against c.n. 12 diameter of the M component, D_M, for L components indicated on scales and identified by symbols: +, Pb; ▽, Sn; ×, Ge; ○, Ga; △, Si. Full lines drawn with slope 1.65 link M components (named) with the same valency. –·–, Slope of a against D_M for rare-earth phases. Inset, bottom right: lattice parameter a against D_L at a constant D_M value of 3.2 Å and M valency of 3, for the L components indicated. Symbols indicate valency: □, 2; ○, 3; ×, 4; △, 5.

There also appears to be a valency effect in respect of the L components with the $Si_3Mn_5X_x$ structure. The insets for figures 21 and 22 show that for phases of L components with valency two, three and four, both a and c against D_L are collinear, but phases with L atoms of valency five lie on a different line. The c.n. 12 D_L values for the atoms of valency five are based on bonding

by three valency orbitals, or a valency of three, in their elemental structures from which their c.n. 12 diameters have been determined, whereas in the $L_3M_5X_x$ phases five valency electrons are used in bonding orbitals. Thus a valency effect is apparent in respect of these phases, although none is found for the phases of L atoms with valency two, three and four, since the number of bonding electrons is of necessity the same as in the elemental structures from which their c.n. 12 diameters were determined. The correctness of this explanation can be demonstrated quantitatively, since calculation of change of valency from three to five for the L atoms, indicates

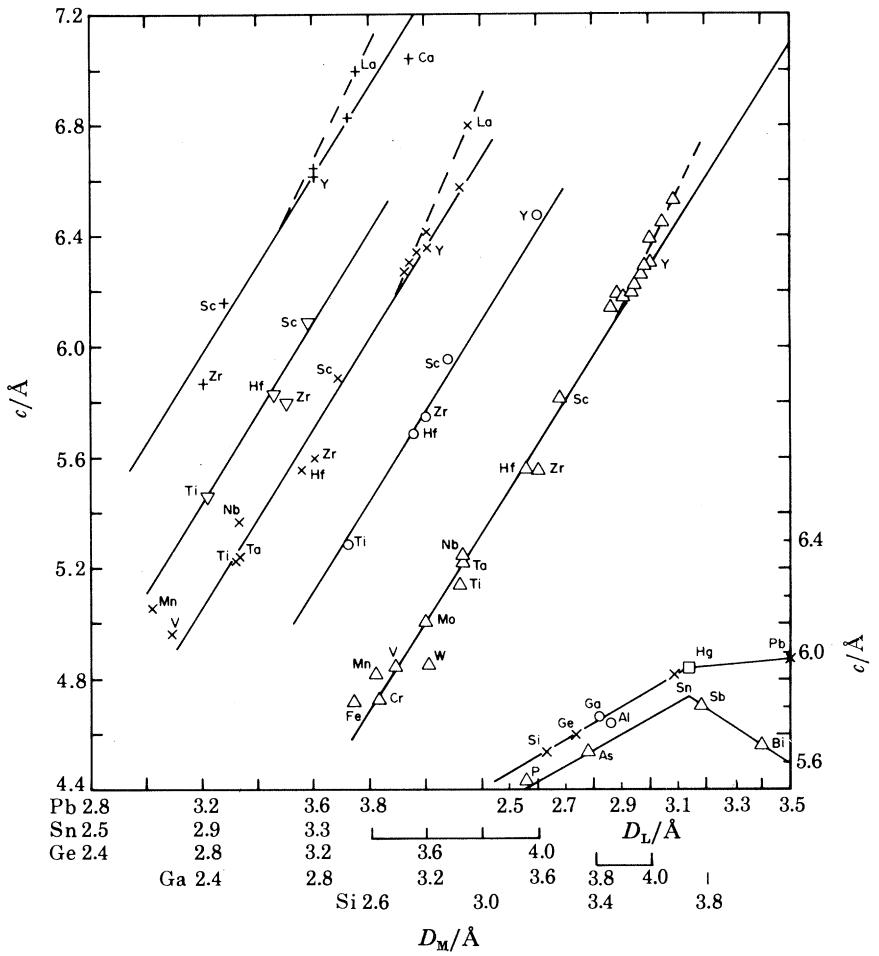

FIGURE 22. As figure 21, except that the c parameter is involved, and the slope of the full lines is 1.6.

D_L values 0.13 Å shorter than their elemental D_L values. Displacement of the line for L atoms of valency five, to D_L values 0.13 Å smaller, in figures 21 and 22 places it on the line for phases with L atoms of valency two to four, where no valency effect occurs!

A similar situation is found in non-interstitial phases with the NaCl structure and L components P, As, Sb, Bi, S, Se, Te and Po. Plots of a against D_L reveal the Group V phases lying on one line and the Group VI phases lying on another line (figure 23). The explanation is similar to that for $Si_3Mn_5X_x$ phases in that the elemental c.n. 12 D_L values are determined from structures with trivalent Group V atoms and divalent Group VI atoms, whereas in the NaCl structure the Group V atoms use five valency electrons and the Group VI atoms use six in six orbitals. Calcu-

lation of the difference between change of diameter for c.n. 12 from valency three to five, and valency two to six gives 0.153 Å, which should be the decrease applied to the elemental D_L values for the Group VI phases to make them collinear with the Group V phases. Applying this shift to the D_L values for the Group VI phases, does indeed make the phases of both Groups collinear.

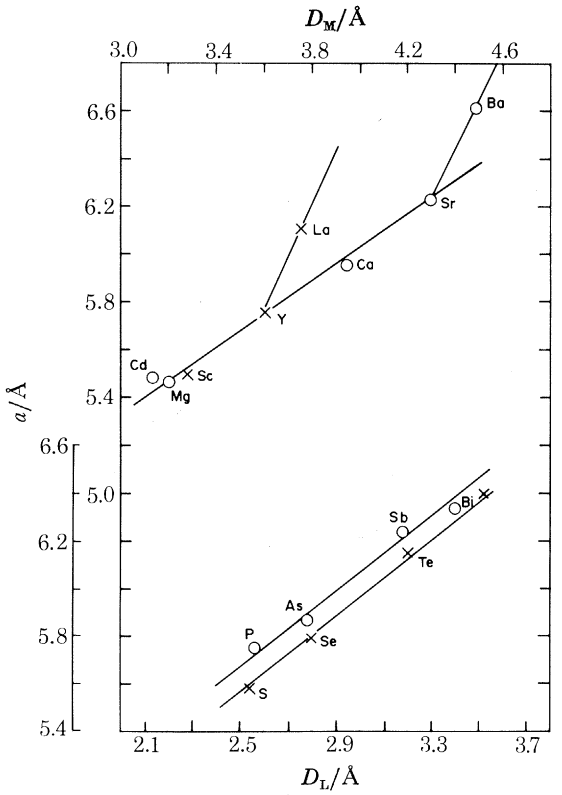

FIGURE 23. NaCl structure, ML. Upper: lattice parameter a against D_M at a constant D_L value of 2.8 Å. M components are named on the diagram. Lower: lattice parameter a of rare-earth alloys against D_L at a constant D_M value of 3.6 Å. L components are named on the diagram.

The calculated change of D_L for Group V phases to a line for phases formed by Group II, III and IV L atoms that should show no valency effect, is 0.13 Å. Unfortunately the only phases of Group IV L atoms with the NaCl structure, are those of the interstitial carbon atoms, or are formed with Group V and VI atoms. Also there are no data for phases of Group II or III L atoms, with M atoms of diameter near 3.6 Å, the constant D_M value at which a values are taken for plotting against D_L. Thus it is not possible to know very accurately the a value to use for phases with Group II and III L atoms. Nevertheless, by extrapolating to $D_M = 3.6$ Å such data as there are, by using a slope of $1.0D_M$, gives a point about 0.10 Å away from the a against D_L line for Group V L atoms, compared to the calculated value of 0.13 Å. This is in reasonable agreement considering the uncertainty of the a against D_M extrapolation. However, it should be noted in figure 23 that the Group II and Group III phases (here the M components) do indeed lie on the same line, revealing no valency effect, as expected, there being no difference between their valency in the NaCl structure and in the elemental structures from which their c.n. 12 diameters were determined.

7. Phases with the $AlCr_2C$ structure

As a final example of the results of this method of analysis of the cell dimensions of intermetallic phases, we shall consider phases with the hexagonal $AlCr_2C$ structure, LM_2C, the dimensional behaviour of which (figures 24–26) is quite different from that of other structures examined. In particular, the a and c dependences on D_L undergo a dramatic change in the region where

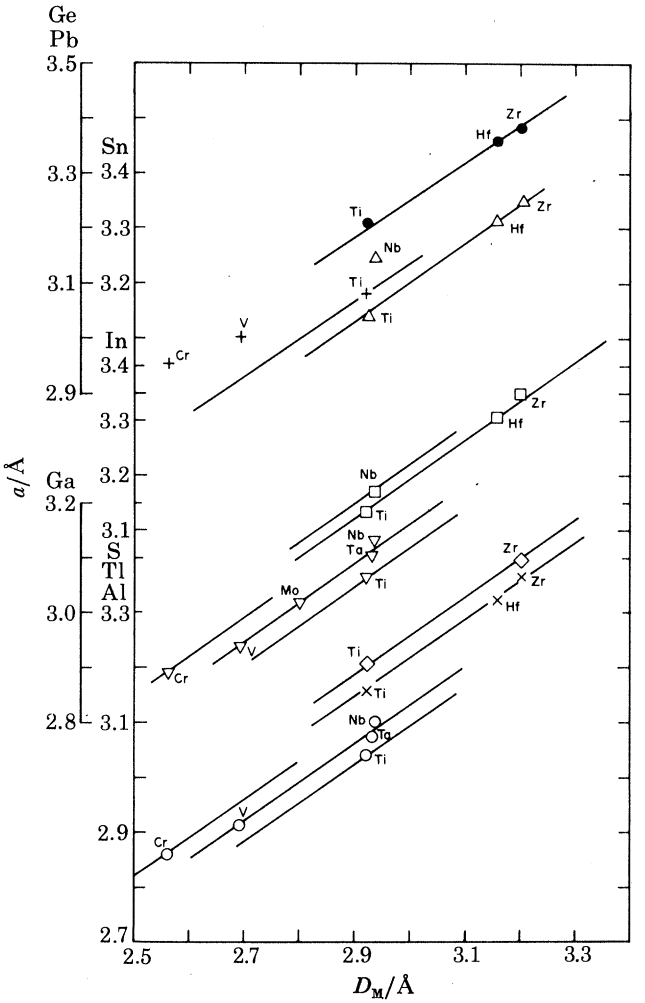

Figure 24. Carbide phases with the $AlCr_2C$ structure, LM_2C. Lattice parameter a against the c.n. 12 diameter, D_M, of the M components named on the diagram. Full lines with slope 0.7 pass through phases with M components with four, five, or six outer electrons. Symbols identify different L components, which are also indicated on the various scales. +, Ge; ●, Pb; △, Sn; □, In; ▽, Ga; ◇, S; ×, Tl; ○, Al.

$a = D_L$; negative dependences of a and c on D_L are observed, and the dependence of c on $6.5\,D_L$ is much greater than could arise through direct contacts with the L atoms in the structure. Also, as already noted, the a and c dependences on D_M exhibit a valency effect involving the transition metal, M atoms.

The data shown in figures 24–26 are represented by (10)–(13).

When $a > D_L$:

$$a = 0.70D_M - 0.65D_L + 0.019S + 2.833, \quad (10)$$

$$c = 3.0D_M + 6.5D_L + 0.072S - 13.798 \quad (11)$$

and additions of $0.9D_L - 2.560$ to (10) and of $-8.15D_L + 24.610$ to (11) give (12) and (13), that apply when $a < D_L$:

$$a = 0.70D_M + 0.25D_L + 0.019S + 0.273; \quad (12)$$

$$c = 3.0D_M - 1.65D_L + 0.072S + 10.812, \quad (13)$$

where S represents the valency effect and has values 0, 3 and 5 for Group IV, V and VI M components respectively. The values of S are selected so as to make the valency effect zero for the Group IV metals, for reasons discussed below (Pearson 1980*e*).

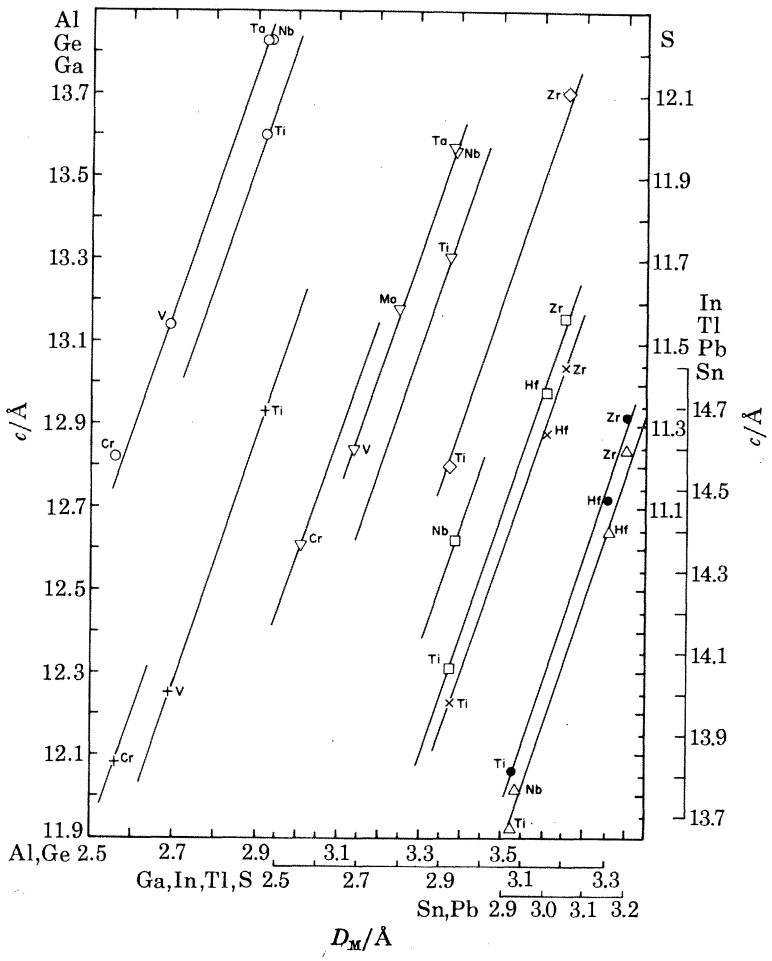

FIGURE 25. As figure 24, except that the c parameter is involved and the slope of the full lines is 3.0.

With the exception of the c values of three sulphur phases, these equations reproduce the observed a values of the twenty-eight known carbide phases that do not have Sn as the L component, to within $|0.015|$ Å, or 0.5 % of the observed values and the c values to within $|0.033|$ Å or 0.26 %, as seen from table 4. The slight disagreement of the calculated and observed c parameters of the SM_2C phases, results from a valency effect involving the sulphur atom; its S^{VI}

diameter for c.n. 12 (2.26 Å) is appropriate for these phases, rather than its S^{II} diameter for c.n. 12 (2.54 Å) determined from its elemental structure. This is apparent from a comparison of the M–L distances against D_L for LTi_2C phases, although it is not more apparent than this slight discrepancy in analysis of the cell dimensions against D_M and D_L because, as shown below, a and c do not depend intrinsically on the diameter of the L component.

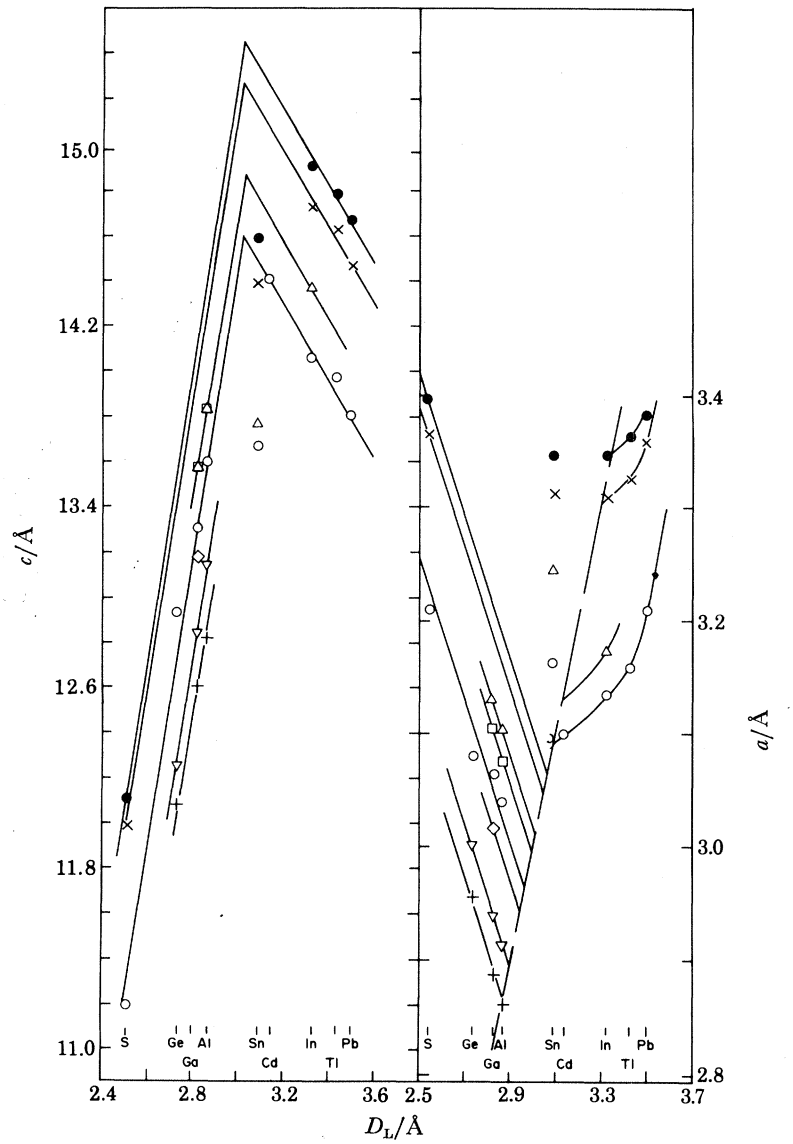

FIGURE 26. Variation of a and of c as a function of D_L for carbide phases with the $AlCr_2C$, LM_2C, structure. M components are identified by symbols: +, Cr; ▽, V; ◇, Mo; ○, Ti; □, Ta; △, Nb; ×, Hf; ●, Zr. The broken line in the right diagram represents $a = D_L$. Note: the scales for a and c are different.

These equations thus show that effective analysis of structural dimensions based on c.n. 12 diameters can be made, regardless of the actual coordinations of the atoms in the structure. It now remains to determine the reason for these dependences.

In the $AlCr_2C$ structure shown in figure 27, there are triangular networks of M atoms in (0001) planes at $\pm z$ and $\frac{1}{2} \pm z$ (z is the fractional coordinate of the M atoms along c) which form layers of

TABLE 4. OBSERVED AND CALCULATED LATTICE PARAMETERS OF $AlCr_2C$ STRUCTURE PHASES LM_2C

	a_{obs}/Å	$(a_{calc}-a_{obs})$/Å	c_{obs}/Å	$(c_{calc}-c_{obs})$/Å
		$a > D_L$		
STi_2C	3.210	0.019	11.20	0.28
$GeTi_2C$	3.079	0.021	12.93	−0.16
$GaTi_2C$	3.064	−0.018	13.305	0.012
$AlTi_2C$	3.04	−0.022	13.60	−0.01
SHf_2C*	~ 3.365	0.029	~ 11.99	0.20
SZr_2C	3.396	0.029	12.11	0.21
GeV_2C	3.001	−0.007	12.25	0.04
GaV_2C	2.938	0.002	12.84	0
AlV_2C	2.913	−0.001	13.14	−0.03
$GaNb_2C$	3.131	−0.020	13.565	0.004
$AlNb_2C$	3.103	−0.020	13.83	0.01
$GaTa_2C$	3.104	0.006	13.57	−0.01
$AlTa_2C$	3.075	0.007	13.83	0.01
$GeCr_2C$	2.954	−0.011	12.08	−0.03
$GaCr_2C$	2.886	0.003	12.61	−0.01
$AlCr_2C$	2.860	0.001	12.82	0.05
$GaMo_2C$	3.017	0.037	13.18	0.13
		$a < D_L$		
$CdTi_2C$	3.099	0.005	14.41	0
$InTi_2C$	3.132	0.020	14.06	0.036
$TlTi_2C$	3.158	0.020	13.98	−0.059
$PbTi_2C$	3.209	−0.014	13.81	−0.001
$InZr_2C$	3.347	0.001	14.91	0.026
$TlZr_2C$	3.363	0.011	14.79	−0.029
$PbZr_2C$	3.384	0.007	14.67	−0.021
$InHf_2C$	3.307	0.010	14.73	0.074
$TlHf_2C$	3.322	0.021	14.63	−0.001
$PbHf_2C$	3.358	0.002	14.47	0.047
$InNb_2C$	3.172	0.045	14.37	−0.02

* Actually $FeHf_2SC_2$.

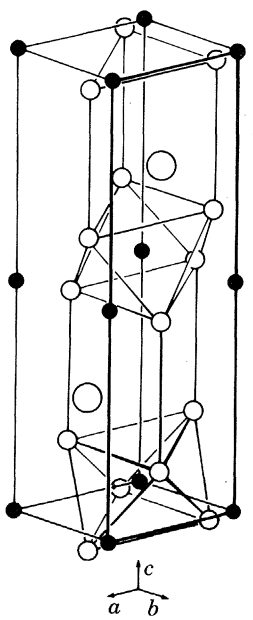

FIGURE 27. Diagrammatic view of the $AlCr_2C$ structure. Large circles, Al; small circles Cr; filled circles, C atoms. Two octahedra and two uncentred trigonal prisms are indicated.

PHILOSOPHICAL TRANSACTIONS OF THE ROYAL SOCIETY A MATHEMATICAL, PHYSICAL & ENGINEERING SCIENCES

edge-sharing octahedra that are centred by C atoms at $z = 0$ and $\frac{1}{2}$. On their other sides, these networks of M atoms form layers of contiguous trigonal prisms, alternate prisms being centred by L atoms at $z = \frac{1}{4}$ and $\frac{3}{4}$. Apart from the axial ratio, the only variable parameter in the structure is the z of the M atoms that allows their movement in the [0001] direction. All of the M and L atoms are located at fixed x and y positions of $\pm(\frac{1}{3}, \frac{2}{3})$. Thus any constraints in their atomic contacts are liable to be reflected directly in changes of the a cell-dimension.

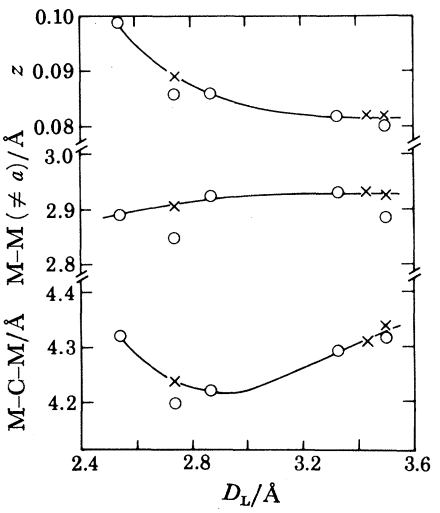

FIGURE 28. LTi_2C phases with the $AlCr_2C$ structure. The z-parameter of the M atoms and the calculated M–M ($\neq a$) and M–C–M distances are plotted against D_L. ○, Data of experimentally determined z-values; ×, data of adjusted z-values.

Accounting for the a and c dependences on $0.7D_M$ and $3.0D_M$, respectively, presents no difficulties. They arise from the arrays of –M–L–M–M–L–M– contacts running throughout the structure (possibly with M–C–M replacing M–M) which involve one diameter of the M atom along a and four diameters of the M atom along c. The resolved components of these contacts along a and c suggest D_M dependences much like those observed. However, the dependence of c on $6.5D_L$ in the region where $a > D_L$, cannot possibly arise intrinsically from direct contacts with the L atoms; it must come from other constraints in the structure.

To account for this D_L dependence, and the driving force that gives rise to it, it is necessary to know the z values for the phases, but very few of these have been determined – let alone accurately. In an attempt to establish the variation of z with D_L, the eight LTi_2C phases were chosen as the most promising. The z value for STi_2C has been determined as 0.099 ± 2 from a single-crystal study and approximate values have been given for the Ge, In and Pb phases from X-ray powder data (Pearson 1967). By assuming also a value of 0.086 for $AlTi_2C$, which is the same value as that accurately determined for $AlCr_2C$, figure 28 shows the variation with D_L of (i) the z parameter, (ii) the calculated M–C–M distance and (iii) the six M–M distances not in (0001) planes, and subsequently referred to as the M–M ($\neq a$) distances. It is apparent from figure 28 that the self-consistency of these data can be improved by increasing z for $GeTi_2C$ from 0.086 to 0.089, and probably by increasing the value for $PbTi_2C$ from 0.080 to 0.082, changes that are well within the probable errors of the experimental values.

Figure 28 now reveals that the Ti–Ti ($\neq a$) distance is an invariant feature of the structure, being essentially constant and equal to $D_{\mathrm{Ti}} = 2.924$ Å for c.n. 12, and that the octahedra diagonals Ti–C–Ti are much smaller than the appropriate radius sums. For any given z value and the a value, which changes little with D_{L} in the region where $a > D_{\mathrm{L}}$, the value of c is prescribed by the constant Ti–Ti ($\neq a$) distance, d, since $d = (\frac{1}{3}a^2 + 4z^2c^2)^{\frac{1}{2}}$. Hence the dependence of c on $6.5D_{\mathrm{L}}$ is quantitatively accounted for, although this still does not provide a reason to explain *this* dependence, rather than a normal dependence of $2.0D_{\mathrm{L}}$ or less, which would arise from direct contacts to the L atoms. It is necessary to consider the M–L distances, which also control the cell dimensions, together with the unit-cell volumes. The M–L distances also depend on a, c and z, the latter in a $(\frac{1}{4} - z)$ relation, so that changes of z that increase the M–M distance decrease the M–L distance.

With M–M ($\neq a$) kept at its constant value of 2.924 Å and with the M–L distance held at an appropriate value for the phase concerned, a and c, which are coupled, can still vary widely, although the value of z is now prescribed within fairly narrow limits. However, the wide variation of a and c that is still permitted, causes a wide variation of the value of the unit-cell volume, and ultimately it is obtaining a suitable value of this for the phase that determines the a and c values. Thus, for example, for the $GaTi_2C$ phase, while keeping M–M ($\neq a$) = 2.924 Å and appropriately M–L = 2.800 Å, a, c and z could vary, respectively, from 3.46 Å, 12.0 Å and 0.089, to 2.80 Å, 14.0 Å and 0.087, but the unit-cell volume would change from 126.6 to 95.7 Å^3. The observed atomic volume of 108.2 Å^3 fixes a, c and z at the observed values of 3.064 Å, 13.30 Å and *ca.* 0.087. Thus it is the coupling of a, c and z through the M–M ($\neq a$) and M–L distances, and of a and c through the cell volume, that provides the reason to establish the c dependence on $6.5D_{\mathrm{L}}$.

In the region where $a < D_{\mathrm{L}}$ and a is now in part controlled by the L–L distances in the triangular nets in (0001) planes, the constant Ti–Ti distance of 2.924 Å again couples a, c and z. This coupling, together with that of a and c in providing suitable cell volumes, accounts quantitatively for the observed c dependence on $-1.65D_{\mathrm{L}}$.

The reason for the a parameters of the SnM_2C phases being too large and the c parameters being too small to fit the systematic variation of lattice parameters of all other phases (figure 26) does not appear to be that they lie in the region where $a = D_{\mathrm{L}}$. Rather, it seems that if they did follow these variations, a would be less than D_{M} for the Zr and Hf phases and about equal to it for the Nb and Ti phases. It is to avoid this extra constraint of the M–M contacts directly influencing a that the a axes expand compared to their expected lengths. The concomitant decrease in the lengths of the c axes is the result of a cell-volume effect, since the observed cell volumes of the SnM_2C phases appear to vary regularly with those of other phases, even though their a and c parameters, as a function of D_{L}, do not. Only for the SnM_2C phases does the possibility of $a < D_{\mathrm{M}}$ arise.

The valency effect involving the M atoms can be quantitatively accounted for on the basis that the –M–L–M–M–L–M– arrays of atoms control the cell dimensions, as far as the M atoms are concerned, and that the number of electrons assigned to the M–C contacts is unimportant.

In the region where $a > D_{\mathrm{L}}$, the M atoms have 3M, 3L and 3C close neighbours for c.n. 9, and the L atoms have 6M neighbours. The numbers of electrons required for the three M–M and three M–L bonds are calculated from the average observed distances, the appropriate radius sums for c.n. 9 or c.n. 6 and Pauling's (1947) equation $R(1)–R(n) = 0.3 \lg n$, for the four LTi_2C, three LV_2C and three LCr_2C phases to give 0.328, 0.311 and 0.310 electrons per bond, respectively. These are to be compared with $\frac{4}{12} = 0.333$, $\frac{5}{12} = 0.417$ and $\frac{6}{12} = 0.500$ electrons per bond, respectively, for the elemental structures of Ti, V and Cr corresponding to their c.n. 12 radii. Thus

it is seen that there is no valency effect for the Ti phases since the number of electrons per bond controlling the cell edges of the LTi_2C phases is the same as in elemental Ti, but there is a valency effect involving the V and Cr phases. Calculations based on these values show that the lines in figures 24 and 25 for the V and Cr phases should be displaced, respectively, by 0.072 and 0.121 Å to lower D_M values than those for the Ti phases, whereas the observed average displacements of a and c for the four Al and Ga phases of V and Cr are 0.070 and 0.115 Å. Similar calculations comparing LZr_2C and LHf_2C phases with LNb_2C and LTa_2C, although involving different electron numbers, give an identical result, as observed, that the Group V metal phases should be displaced by 0.073 Å to lower D_M values than the Group IV metal phases. Thus the valency effect is generally accounted for and shown to be essentially zero for the Group IV transition metal phases.

The remaining transition-metal electrons not used in the six M–M and M–L bonds are assigned to bands derived from carbon 2p states and transition metal 3d states (non-bonding). Since these bands probably overlap slightly (cf. Neckel *et al.* 1976), the p bands can receive approximately two electrons per transition metal atom. With approximately two electrons per Group IV transition metal assigned to M–M and M–L bonds, the remainder go to the p bands so all electrons are bonding, and there is no valency effect. However, with the Group V and VI metals, some electrons must be assigned as non-bonding in d bands and so the valency effect arises.

The Ti, Zr, Hf, Nb and Ta phases are all true Hägg interstitial phases with $R_C/R_M < 0.59$, and for the Group IV metals M–M ($\neq a$) $= D_M$ for c.n. 12, whereas it is just slightly larger for the Nb and Ta phases (average 0.038 Å larger), so that transition metal d bands clearly form. However, the V and Cr phases are not true interstitial phases since $R_C/R_M > 0.59$, and the average observed M–M ($\neq a$) distances are distinctly larger (0.111 and 0.187 Å) than the c.n. 12 atomic diameters. Thus it is apparent that the M–C–M distances increase the M–M distances in the V and Cr phases, and whether the transition metals still form d bands is perhaps uncertain. Nevertheless the analyses are significant in showing that in a hexagonal interstitial phase where two degrees of freedom – the axial ratio, c/a, and the z parameter of the M atoms – would have permitted any symmetrical mode of distortion of the interstitial octahedra as the relative sizes of the M and L components change in a series of phases, the observed invariance of the M–M ($\neq a$) distance is the only condition that would maintain three-dimensional d bands throughout the layers of octahedra (Pearson 1980*e*).

This treatment of phases with the $AlCr_2C$ structure provides an example of the extension of the method of analysis from binary phases to a ternary phase when one of the components, here carbon, is the same in all alloys considered. This is quite permissible, provided that any extra conditions introduced through the presence of the third component are taken into account. In this case the extra condition was an interaction between M atoms at opposite apexes of the octahedra, via the interstitial carbon atoms. Consideration of the direct distances between such pairs of M atoms in a binary phase would indicate no such interaction.

8. Conclusions

(*a*) The method of analysing the unit-cell dimensions of binary metallic phases with a given crystal structure, described in this paper, appears to avoid the analytical difficulties that normally arise from the uncertainty about atomic size because of the coordination numbers and valency of the atoms in the phases concerned. The method uses measured lattice parameters to

identify atomic arrays that control the cell dimensions, and thereafter appears capable of deducing quantitative geometrical and electronic information not previously available.

(*b*) It is shown that the unit-cell dimensions of binary phases with a given crystal structure generally depend linearly on the elemental c.n. 12 diameters, D_M and D_L, of the component atoms, regardless of the actual coordination number(s) of the atoms in the structure. A linear dependence of the cell dimensions on the valency of one of the component atoms may also occur, if its average number of electrons per bond, adjusted to c.n. 12, differs from that in the elemental structure from which its c.n. 12 diameter was derived – provided that the appropriate atomic arrays control the cell dimensions. The reason why differences of valency compared to the elemental structure, but not differences of coordination compared to c.n. 12, appear in the analyses is that the differences of coordination are the same for all phases with the structure examined, whereas the differences of valency change with the valency of the component atoms.

(*c*) The linear equations relating unit-cell dimensions to D_M and D_L (and valency) permit the explicit determination of the arrays of atomic contacts in the structure, that control the cell dimensions. Generally the equations also reproduce the observed cell dimensions to a high degree of precision and permit the accurate prediction of cell dimensions of new phases, provided that they follow the same dimensional constraints as those on which the equations are based.

(*d*) Although numerous investigations have shown that particular systems of atomic radii, can be applied to metallic phases with a given structure, this study is perhaps the first to show to what extent a general system of metallic diameters (here for c.n. 12) can be usefully applied to intermetallic phases. This is because, as noted in (*a*) the method can reveal whether the valency and/or number of bond orbitals of atoms in phases the structures of which are examined, are the same as those in the elemental structures used to derive the atomic diameters.

(*e*) Finally, the analyses based on measured cell dimensions, have thereafter provided new information regarding: (i) the reason for the very constant axial ratios observed for phases with certain uniaxial crystal structures, (ii) the significance of fixed or variable atomic coordinates in relation to unit-cell dimensions, (iii) differences in the atomic arrays that control the cell dimensions of many rare-earth phases, compared to those of phases with the same crystal structure that do not contain rare-earth atoms, and (iv) the electronic interactions in true Hägg interstitial phases, particularly in non-cubic structures where the interstitial octahedra can be distorted in various modes as the relative sizes of the component atoms change.

This work was supported by a grant from the Natural Sciences and Engineering Research Council of Canada.

References

Brewer, L. 1965 In *High strength materials* (ed. V. K. Zackay), pp. 12–103. New York: Wiley.
Brunner, G. O. 1977 *Acta crystallogr.* A **33**, 226–227.
Carter, F. L. 1978 *Acta crystallogr.* B **34**, 2962–2966.
Hägg, G. 1929 *Z. phys. Chem.* B **6**, 221.
Hägg, G. 1931 *Z. phys. Chem.* B **12**, 33, 413.
Johnson, Q., Smith, G. S. & Wood, D. H. 1969 *Acta crystallogr.* B **25**, 464–469.
Neckel, A., Rastl, P., Eibler, R., Weinberger, P. & Schwarz, K. 1976 *J. phys. Chem.* C **9**, 579–592.
Pauling, L. 1947 *J. Am. chem. Soc.* **69**, 542–553.
Pearson, W. B. 1967 *A handbook of lattice spacings and structures of metals and alloys*. Oxford: Pergamon Press.
Pearson, W. B. 1972 *The crystal chemistry and physics of metals and alloys*. New York: Wiley–Interscience.
Pearson, W. B. 1979*a* *Acta crystallogr.* B **35**, 1329–1333.
Pearson, W. B. 1979*b* *Proc. R. Soc. Lond.* A **365**, 523–535.

PHILOSOPHICAL TRANSACTIONS OF THE ROYAL SOCIETY A MATHEMATICAL, PHYSICAL & ENGINEERING SCIENCES

Pearson, W. B. 1980*a* *Z. Kristallogr.* **151**, 301–315.
Pearson, W. B. 1980*b* *Z. Kristallogr.* **152**, 23–36.
Pearson, W. B. 1980*c* *J. less-common Metals.* **71**, 85–104.
Pearson, W. B. 1980*d* *J. less-common Metals.* **72**, 107–124.
Pearson, W. B. 1980*e* *Acta crystallogr.* A **36**, 724–732.
Sato, H. & Toth, R. S. 1968 *Bull. Soc. fr. Minér. Cristallogr.* **91**, 557–574.
Slater, J. C. 1962 Solid State and Molecular Theory Group, M.I.T. Q.P.R. No. 46, p. 6.
Teatum, E., Gschneidner, K. & Waber, J. 1960 LA-2345. U.S. Department of Commerce, Washington, D.C.
Zachariasen, W. H. 1973 *J. inorg. nucl. Chem.* **35**, 3487–3497.

PHILOSOPHICAL TRANSACTIONS OF THE ROYAL SOCIETY A MATHEMATICAL, PHYSICAL & ENGINEERING SCIENCES